creative commons
COMMONS DEED

저작자표시-비영리-변경금지 2.0 대한민국

이용자는 아래의 조건을 따르는 경우에 한하여 자유롭게

- 이 저작물을 복제, 배포, 전송, 전시, 공연 및 방송할 수 있습니다.

다음과 같은 조건을 따라야 합니다:

저작자표시. 귀하는 원저작자를 표시하여야 합니다.

비영리. 귀하는 이 저작물을 영리 목적으로 이용할 수 없습니다.

변경금지. 귀하는 이 저작물을 개작, 변형 또는 가공할 수 없습니다.

- 귀하는, 이 저작물의 재이용이나 배포의 경우, 이 저작물에 적용된 이용허락조건을 명확하게 나타내어야 합니다.
- 저작권자로부터 별도의 허가를 받으면 이러한 조건들은 적용되지 않습니다.

저작권법에 따른 이용자의 권리는 위의 내용에 의하여 영향을 받지 않습니다.

이것은 이용허락규약(Legal Code)을 이해하기 쉽게 요약한 것입니다.

Disclaimer

dCollection

Ph.D. Dissertation of Medicine

Polo-like kinase 1 regulates chromosomal instability and paclitaxel resistance in breast cancer cells

유방암 항암제 내성 관련 PLK1 유전자의 기전 연구

February 2023

Graduate School of
Seoul National University College of Medicine
Interdisciplinary Programs in Cancer Biology

Mingji Quan

Polo-like kinase 1 regulates chromosomal instability and paclitaxel resistance in breast cancer cells

Advisor Hyeong-Gon Moon

Submitting a Ph.D. Dissertation of Medicine

October 2022

Graduate School of
Seoul National University College of Medicine
Interdisciplinary Programs in Cancer Biology

Mingji Quan

Confirming the Ph.D. Dissertation written by
Mingji Quan
January 2023

Chair	Hak Chang	(Seal)
Vice Chair	Hyeong-Gon Moon	(Seal)
Examiner	Jong-Il Kim	(Seal)
Examiner	Han-Byoel Lee	(Seal)
Examiner	Jeong Eon Lee	(Seal)

Abstract

Chromosomal instability (CIN) contributes to intercellular genetic heterogeneity and has been implicated in paclitaxel (PTX) resistance in breast cancer. In this study, I explored polo-like kinase 1 (PLK1) as an important regulator of mitotic integrity and as a predictive biomarker for PTX resistance in breast cancer.

In Chapter 1, provides a general overview of anti-cancer drug resistance and cell heterogeneity. PTX is a commonly used cytotoxic chemotherapeutic agent for triple-negative breast cancer (TNBC). PTX causes cancer cell death by stabilizing microtubules and inducing multinucleation and cell cycle arrest. Emerging evidence suggests that CIN in breast cancer might serve as a predictor of PTX response. Furthermore, extensive published data have shown that CIN is associated with various malignant features in multiple types of human cancers. Of note, recent studies have shown that CIN is also associated with PTX sensitivity in breast cancer, although varying results suggest that there may be an optimal threshold of CIN for tumor progression, beyond which further CIN may be deleterious for cancer cell survival. However, detailed studies exploring potential nonlinear relationships between

CIN and therapeutic resistance in breast cancer are lacking.

In Chapter 2, genes related to PTX resistance are identified through a kinome-wide CRISPR/Cas9 screen in breast cancer cells. Among the top candidate genes identified, PLK1 was chosen for further experiments. *In vitro* cell proliferation and apoptosis assays were performed to determine the effects of PLK1 inhibition on breast cancer cells. PLK1 knockdown inhibited the proliferation of MDA-MB-231 and MDA-MB-468 cells *in vitro*. Moreover, PLK1 silencing sensitized breast cancer cells to PTX. PLK1 upregulation in primary breast cancer tumors was associated with decreased overall patient survival based on the analysis of The Cancer Genome Atlas (TCGA) and Molecular Taxonomy of Breast Cancer International Consortium (METABRIC) databases. Lower PLK1 expression levels were associated with increased response to neoadjuvant chemotherapy (NAC) in breast cancer. Data from these studies suggest targeting PLK1 may be an effective treatment strategy for PTX-resistant breast cancer. Overall, PLK1 levels served as an independent predictor of PTX-based NAC response in breast cancer.

In Chapter 3, the mechanistic role through which PLK1 regulates

CIN and PTX resistance was further explored in breast cancer cells. RNA-sequencing (RNA-Seq) analysis revealed that PLK1 depletion leads to changes in gene expression signatures associated with chromosome missegregation. Immunofluorescence microscopy was used to measure the degree of multipolar cell division. Silencing of PLK1 induced the formation of multipolar spindles and increased the percentage of multipolar cells. In addition, PLK1 silencing resulted in the downregulation of BubR1 and Mad2, which are key regulatory proteins for spindle assembly checkpoint (SAC) activity in prometaphase. Furthermore, kinetochore localization of BubR1 was significantly reduced in PLK1-silenced breast cancer cells. In addition, PLK1 knockdown inhibited the proliferation of MDA-MB-231 and MDA-MB-468 cells *in vivo* and sensitized mouse xenograft tumor models to PTX cytotoxicity. In agreement with *in vitro* experiments, PLK1-silenced xenograft tumors showed significantly increased multipolar spindles similar that of PTX-treated xenograft tumors. In conclusion, PLK1 promotes multipolar spindle formation, which can lead to increased PTX sensitivity.

Keyword: Breast cancer, CRISPR/Cas9, Paclitaxel, PLK1, Spindle Poles, Chromosomal instability

Student Number: 2020-35134

Table of Contents

List of Figures

Chapter 3.

List of Abbreviations

FDR; False Discovery Rate

NGS; Next-Generation Sequencing

PLK1; Polo-Like Kinase 1

PTX; Paclitaxel

sgRNA; single-guide RNA

IC_{50}; half maximal inhibitory concentration

MTT; thiazolyl blue tetrazolium bromide

ns; non-significant

qPCR; qualitative Polymerase Chain Reaction

siRNA; small interfering RNA

sh-CTL; non-targeting shRNA

DAPI; 4′,6-diamidino-2-phenylindole

SD; Standard Deviation

METABRIC; Molecular Taxonomy of Breast Cancer International Consortium

TCGA; The Cancer Genome Atlas

SAC; Spindle Assembly Checkpoint

BubR1; Bub1-related kinase

Mad2; Mitotic arrest deficient 2

NAC; Neoadjuvant Chemotherapy Response

CIN; Chromosome instability

CI; Combination Index

TNBC; Triple-negative breast cancer

FACS; Fluorescence Activated Cell Sorting

GO; Gene Ontology

KEGG; Kyoto Encyclopedia of Genes and Genomes

RECIST; Revised Response Evaluation Criteria in Solid Tumors

Chapter 1. General Introduction

Breast cancer was the most commonly diagnosed cancer globally in 2020 [1] and is the leading cause of cancer-related deaths in women [2]. Breast cancer is highly heterogeneous with diverse molecular features that can be classified into several subtypes [3]. Molecular classification of breast tumors is important for assessing patient prognosis and determining the best treatment options [4]. Among the clinical breast cancer subtypes, triple-negative breast cancer (TNBC) is the most aggressive and has the highest risk of recurrence and death [4, 5]. Patients with TNBC are often treated with cytotoxic chemotherapy in addition to localized radiation or surgery [4, 6, 7].

Paclitaxel (PTX) is a commonly used cytotoxic chemotherapeutic agent used in the clinic to treat TNBC [6, 7]. PTX induces cancer cell death by stabilizing microtubules and inducing multinucleation and cell cycle arrest [8, 9]. However, most patients with TNBC that metastasizes eventually develop resistance to PTX and show disease progression [10]. Although several mechanisms of PTX resistance have been identified in breast cancer, such as alterations to tubulin structures, defects in the spindle assembly checkpoint

(SAC), and dysregulation of several proteins like P-glycoprotein and TP53, strategies to overcome these mechanisms remain challenging [8, 10-12]. Emerging evidence suggests that chromosomal instability (CIN) in breast cancer might serve as a predictor of PTX response [8, 9, 12, 13]. Furthermore, recent studies report associations between CIN and various malignant features in several types of human cancer [14, 15].

CIN is observed in many human tumors and results from chromosome missegregation during mitosis, leading to numerical and structural chromosomal abnormalities in the resulting daughter cells [15]. Although CIN is common in tumors and correlates with chemoresistance, metastasis, and poor prognosis, its role in tumor evolution is complex and nuanced [16]. For instance, high levels of CIN predict increased sensitivity to cytotoxic therapies including 5-Fluorouracil and cisplatin in ovarian and breast cancer [12, 17-19]. However, conflicting results demonstrating the opposite effect suggest that there is an optimal level of CIN that promotes tumor progression; CIN above this threshold may be deleterious for cancer cell survival [20].

Kinases often perform critical cellular functions that cancer cells

require to proliferate and metastasize [21]. Recent technical advances, such as CRISPR/Cas9, have enabled comprehensive screening of the kinome, the entire cellular collection of kinases, to identify therapeutic targets for cancer [22]. In fact, kinome-wide screening has identified key kinases that mediate PTX resistance in ovarian and breast cancer [23, 24].

In the present study, I identified polo-like kinase 1 (PLK1) as a potential regulator of PTX resistance in breast cancer using CRISPR/Cas9-based kinome screening. My data also demonstrated that PLK1 can modulate the response to PTX by regulating CIN in breast cancer cells.

Chapter 2.
Kinome CRISPR/Cas9 screening for paclitaxel resistance in breast cancers

Introduction

The CRISPR-Cas9 genome editing system is a useful tool to screen for drug resistance genes in cancer. In a melanoma model, Shalem et al. showed that a genome-scale CRISPR-Cas9 knockout library screening for genes successfully identified several targets important for vemurafenib resistance [25]. In addition, Wang et al. conducted a CRISPR-Cas9 screen using a genome-wide sgRNAs library in hematological tumor cell lines and found that TOP2A or CDK6 are important drug resistance genes [26]. Furthermore, CRISPR/Cas9 screening has also been used to study genes related to PTX, cisplatin, and carboplatin drug resistance in lung cancer [27-30]. Collectively, these studies demonstrate that CRISPR/Cas9 screening is an accepted methodology to screen for factors that contribute to cancer chemotherapy resistance and identify novel drug targets for cancer therapy.

PLK1 is a serine/threonine-protein kinase that plays multiple roles in the cell cycle. Specifically, PLK1 is important for regulation of

mitotic entry, progression through the G2/M checkpoint, centrosome coordination, spindle assembly, chromosome segregation, and DNA replication [31]. PLK1 is highly expressed in many types of cancer [32], including TNBC [33]. PTX is a cytotoxic microtubule-targeting agent that stabilizes microtubules, suppresses tubulin dynamics, and induces mitotic arrest, resulting in apoptotic cell death [10].

According to international guidelines, neoadjuvant chemotherapy (NAC) has become the standard therapy for locally advanced TNBC; it is an alternative option for primary operable TNBC [34]. TNBC patients showed significantly higher response rates to taxane-based NAC than did patients with other breast cancer subtypes. It is estimated that 30%-40% patients with TNBC who have achieved pathologic complete response(pCR) after NAC. Additionally, pCR is strongly associated with long-term survival outcomes [35]. Nevertheless, many TNBC patients do not achieve pCR and relapse with drug-resistant disease. Therefore, additional research is greatly needed to identify factors that promote PTX resistance in TNBC to improve patient outcomes.

Materials and Methods

Breast cancer cell lines and small interfering RNA (siRNA) treatment

Breast cancer cell lines were purchased from the Korean Cell Line Bank (Seoul, Korea). MCF10A and MDA-MB-453 cells were obtained from the American Type Culture Collection (ATCC; Manassas, USA). Non-tumorigenic mammary epithelial MCF10A cells were cultured in a 1:1 mixture of Dulbecco's modified Eagle's medium (DMEM; Biowest, Riverside, USA) and Ham's F12 medium (Biowest), containing 5% horse serum (Gibco, Waltham, USA), 20 ng/mL epidermal growth factor (EGF; Sigma-Aldrich, St. Louis, USA), 10 μg/mL insulin (Sigma-Aldrich), and 500 ng/mL hydrocortisone (Sigma-Aldrich). MCF7, MDA-MB-231, MDA-MB-468, HS578T, T47D, and normal human lung fibroblast WI38 cells were cultured in DMEM supplemented with 10% fetal bovine serum (FBS; Gibco) and 1% penicillin/streptomycin (Gibco). SK-BR3, ZR-75-1, BT474, MDA-MB-453, BT20, HCC38, and HCC70 cells were maintained in RPMI 1640 (Biowest) supplemented with 10% FBS and 1% penicillin/streptomycin. For the siRNA experiments, commercially available PLK1 (Gene ID: 5347) siRNA was purchased from Dharmacon Inc. (Lafayette, USA). Cells were

transfected with siRNA (10 nM) using the ON-TARGETplus human PLK1 siRNA-SMARTpool siRNA transfection reagent (Dhamacon Inc.), according to the manufacturer's instructions.

Human kinome CRISPR/Cas9 knockout library screening

Lentiviral particles were produced using HEK293-FT cells as described previously [36]. The human kinome CRISPR/Cas9 pooled library (Addgene #1000000083), psPAX2 (Addgene #12260), and pCMV-VSV-G (Addgene #8454) plasmids were kindly provided by John Doench, David Root, Didier Trono, and Bob Weinberg, respectively [37]. Transduction of the CRISPR lentiviral library into the MDA-MB-231 and MDA-MB-468 cells was performed as previously described [36]. Cells were divided into two groups, with vehicle or PTX (IC20 concentration) and maintained for 14 days. Genomic DNA from residual cells was extracted using the QIAamp DNA Blood Mini Kit (QIAGEN, Hilden, Germany), and single-guide RNA (sgRNA) was amplified by polymerase chain reaction (PCR) with Illumina primers [36]. PCR amplicons were sequenced using the HiSeq 2500 platform (Illumina, San Diego, USA), and sgRNA frequencies were analyzed using the MAGeCK algorithm [38].

Cell viability assay and 3D cell culture

Briefly, cells were seeded into 96-well plates (3×10^3 cells/well) and treated with various concentrations of PTX for 72 hours. The cells were then incubated with 0.5 mg/mL thiazolyl blue tetrazolium bromide (MTT; Sigma-Aldrich) for 3 hours at 37°C. The medium was discarded and 200 μL of dimethyl sulfoxide (Duchefa Biochemie, Harriem, Netherlands) was added to each well to dissolve the formazan crystals in the cells. The absorbance was measured at 570 nm using a microplate reader (BioTek Instruments, Winooski, USA). For 3D cell culture, cells (5×10^3 cells/well) were suspended and seeded in 24-well plates in growth factor-reduced Matrigel (BD Biosciences, San Jose, USA). Spheroid growth and dimensions were measured as previously described [39].

Western blotting and real-time PCR

Cell lysates were harvested using RIPA buffer (Thermo Scientific), protease inhibitor and phosphatase inhibitor (Thermo Scientific). Lysates were incubated for 10 minutes on ice and centrifuged at 14,000 rpm for 15 minutes at 4°C. Protein concentration was measured using a BCA assay kit (Thermo Scientific), separated by sodium dodecyl sulfate-polyacrylamide gel electrophoresis (SDS-PAGE), and transferred to polyvinylidene fluoride (PVDF; Sigma-Aldrich) membranes. After blocking with 5% bovine serum albumin

(BSA; Biosesang, Seongnam, Korea) solution, membranes were incubated with primary antibody overnight at 4℃. The secondary antibody was diluted (1:3,000) in a 5% BSA solution. Western blotting bands were detected using an Amersham Imager 680 (GE Healthcare Life Sciences, Piscataway, USA). The following antibodies were used: β-actin (#sc-47778; Santa Cruz Biotechnology, Dallas, USA), PLK1 (#ab17056; Abcam, Cambridge, UK), Mad2L1 (#ab97777; Abcam), and BubR1 (#ab172584; Abcam).

Total RNA was extracted from the cells using TRIzol reagent (Favorgen , Pingtung, Taiwan). The Prime Script 1st strand cDNA Synthesis Kit (Takara, Osaka, Japan) was used for reverse transcription of RNA, and qPCR assays were performed using Power SYBR Green PCR Master mix (Thermo Scientific). The reactions were performed using an ABI7500 real-time PCR system (Thermo Scientific). To compare the relative mRNA expression levels, the expression levels of PLK1 were normalized to glyceraldehyde 3-phosphate dehydrogenase (GAPDH). The primer sequences were as follows:

PLK1 forward: 5′-CAGCAAGTGGGTGGACTATT-3′, reverse: 5′-GTAGAGGATGAGGCGTGTTG-3′;

GAPDH forward: 5′-TTTCTAGACGGCAGGTCAGG-3′, reverse: 5′-ACCCAGAAGACTGTGGATGG-3′.

Cell apoptosis and cell cycle arrest assay

The cells were seeded into 6-well plates (2×10^5 cells/well) and transfected with siPLK1 in FBS-free DMEM for 6 hours. The cells were then cultured in PTX-containing 10% FBS DMEM at 37°C for 48 hours and stained with annexin V-FITC and propidium iodide (PI; BD Biosciences) according to the manufacturer's instructions. For the analysis of cell cycle arrest, cancer cells were transfected with PLK1 siRNA and treated with PTX as previously described. The cells were then fixed with 75% ethanol and stained with PI at 4°C for 30 minutes. Finally, apoptosis and cell cycle arrest were detected using a BD FACSCanto and a BD FACSCalibur (BD Biosciences).

Efficacy assessment

RECIST version 1.1 [40] was used to evaluate chemotherapeutic efficacy according to validated and consistent criteria to assess changes in tumor burden. Complete response (CR): disappearance of all lesions for >4 weeks; Partial response (PR): ≥30 percent decrease in the sum of the longest diameters; Progress disease

(PD): ≥ 20 percent increase in sum, at least 5mm in the longest diameters; Stable disease (SD): neither PR nor PD.

Statistical analysis

GraphPad Prism version 8.02 (GraphPad Software, San Diego, USA) was used to generate graphs and perform statistical analysis. Data are presented as the mean ± standard deviation (SD) and represent three independent experiments, except for CRISPR/Cas9 screening, 3D spheroid growth, and *in vivo* tumor growth experiments. Student's *t*-tests or Mann-Whitney *U* tests were used to compare the means between the groups. Kaplan-Meier survival analyses were performed using log-rank tests to assess the time to progression and survival.

Results

CRISPR/Cas9-based kinome-wide screening identifies PLK1 as a critical factor for PTX resistance in breast cancer

To search for genes associated with PTX resistance, I conducted kinome-wide CRISPR/Cas9 screening in breast cancer cell lines. A lentiviral sgRNA library was used to knockout 763 human kinases. After lentiviral transduction, MDA-MB-231 and MDA-MB-468 breast cancer cells were treated with vehicle or a 20% concentration of PTX for 14 days. Cells were sequenced on day 0 (no treatment) and day 14 (vehicle- or PTX-treated) and differences in sgRNA frequencies were calculated using the MAGeCK algorithm [38]. Genes important for PTX resistance should theoretically have a lower sgRNA frequency in cells treated with PTX than in those treated with vehicle. The comparison data from day 0 and day 14 for vehicle-treated cells were used to exclude kinases associated with survival fitness for *in vitro* cell survival in the absence of PTX pressure (Figure 1a). I identified 48 and 87 kinase genes from MDA-MB-231 cells and MDA-MB-468 cells, respectively, for which the sgRNA frequencies were decreased by more than half after treatment with PTX compared with vehicle treatment (Figure 1b). A total of 28 (22.9%) out of the

135 genes overlapped in both the cell types. For the comparison between day 0 and day 14 for the vehicle-treated cells, 95 genes showed substantial reduction, with only the ATR gene overlapping between the two cell types (Figure 1c). The 28 genes were significantly enriched with genes involved in cell division, such as the G2M checkpoint or E2F targets (Figure 2a). In addition, reactome pathway analysis (http://reactome.org) revealed several key hub genes among these 28 genes (Figure 2b). Among the key hub genes, PLK1 was selected for further investigation because it showed the largest reduction in MDA-MB-231 cells (Figure 2c).

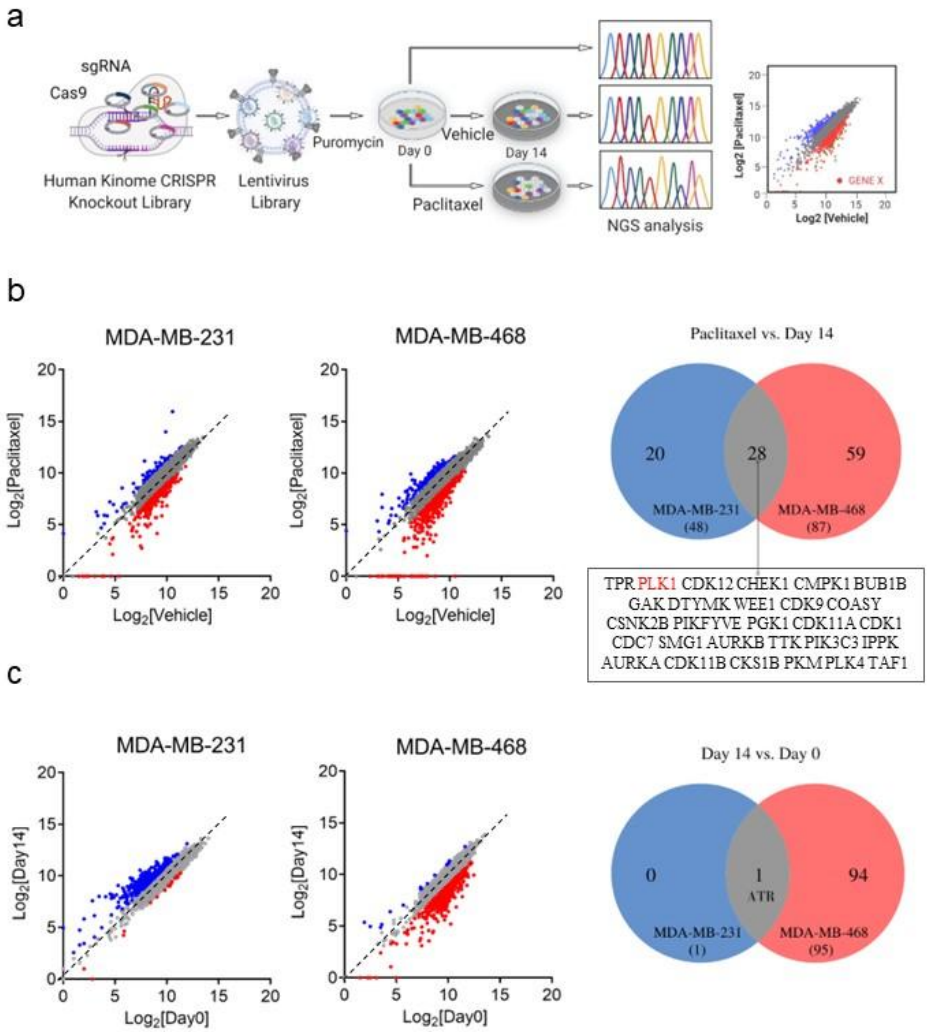

Figure 1. Human kinome CRISPR/Cas9 screening for the identification of candidate therapeutic target genes related to PTX resistance in breast cancer **a.** Schematic illustration showing the human kinome CRISPR/Cas9 knockout screens used to identify genes associated with PTX resistance in MDA-MB-231 and MDA-MB-468 cells **b.** Scatterplots of normalized sgRNA counts for PTX- versus vehicle-treatment at day 14 (left panel). Red dots

show that the sgRNA frequencies were depleted in PTX-treated cells (log2 [fold change] ≤ -1). Venn diagram of 28 genes that overlapped in MDA-MB-231 and MDA-MB-468 cells (right panel) **c.** Scatterplots of normalized sgRNA counts on day 14 versus normalized sgRNA counts on day 0 for cells grown in control media. The Venn diagram of one gene overlapped in MDA-MB-231 and MDA-MB-468 cells (right panel)

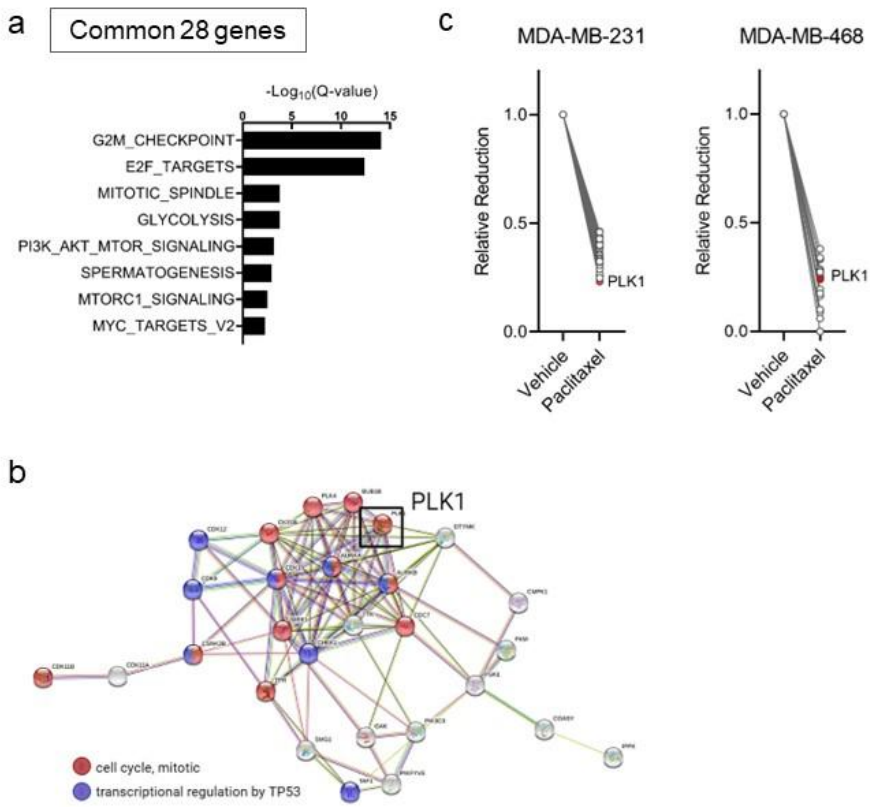

Figure 2. Analysis common 28 genes, selected PLK1 as a candidate gene regulating PTX resistance **a.** Significantly enriched gene sets

(FDR Q < 0.01) for the 28 genes from the PTX-treated group **b.** STRING network analysis of the 28 genes depleted in the PTX-treated group. Genes involved in cell cycle progression and transcriptional regulation by TP53 are indicated in red and blue, respectively. PLK1 indicated by a black box is a one of the hub nodes in the network **c.** Changes in the normalized sgRNA counts in key hub genes between the vehicle- and PTX-treated groups

PLK1 silencing inhibits breast cancer cell growth and sensitizes cells to PTX cytotoxicity

To investigate the role of PLK1 in breast cancer, I first compared PLK1 expression levels between normal mammary epithelial cells (MCF10A) and 10 different breast cancer cell lines. Breast cancer cells showed significant upregulation of PLK1 mRNA and protein expression compared with noncanerous MCF10A cells (Figure 3a and b). Next, I investigated the effect of PLK1 loss on breast cancer cell phenotype *in vitro*. Treatment of cells with siRNA against PLK1 significantly reduced the expression of PLK1 in MDA-MB-231 and MDA-MB-468 cells (Figure 4a). Silencing of PLK1 resulted in a significant reduction in cell viability (Figure 4b) and growth in 3D culture of MDA-MB-231 (Figure 5a). Since PLK1 is a potential regulator of PTX resistance, I evaluated

whether silencing of PLK1 resulted in increased breast cancer cell PTX sensitivity. In both MDA-MB-231 and MDA-MB-468 cells, combining si-PLK1 and PTX resulted in increased cell death compared with PTX treatment alone (Figure 6a and b). The annexin V assay also demonstrated that the combination of si-PLK1 and PTX was associated with increased apoptosis in both cell types (Figure 7a and b), which occurred by inducing G2/M cell cycle arrest (Figure 8a and b). Additionally, silencing of PLK1 resulted in a significant reduction in the IC_{50} value of PTX *in vitro* (Figure 9a and b). A synergistic effect on cancer cell killing was also confirmed between PTX and PLK1 inhibitor volasertib with the combination index (CI) [41] (Figure 10a and b).

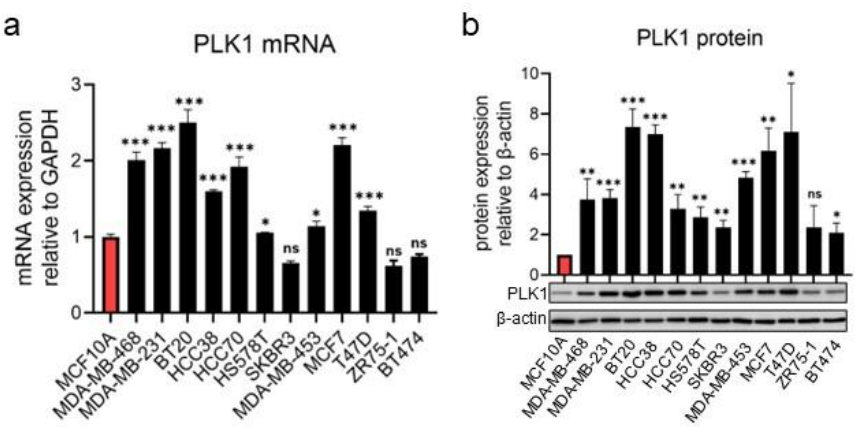

Figure 3. Breast cancer cells of PLK1 mRNA and protein expression compared with MCF10A cells **a, b.** qPCR analysis and

western blotting gel images showing the expression levels of PLK1 mRNA and protein in breast cancer cells and mammary normal epithelial cells. Error bars are mean ± SD; Student's *t*-tests. $*p < 0.05$, $**p < 0.01$, and $***p < 0.001$

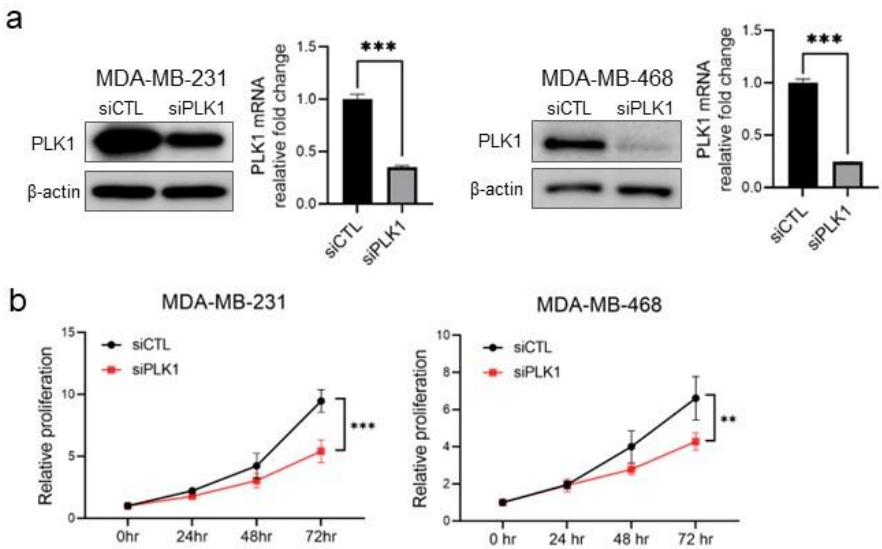

Figure 4. PLK1 knockdown decreased viability of MDA-MB-231 and MDA-MB-468 cells **a.** mRNA and protein levels of PLK1 after siPLK1 treatment **b.** At 72 hours after transfection, cell proliferation was examined using MTT assays. Error bars are mean ± SD; Student's *t*-tests. $**p < 0.01$, and $***p < 0.001$

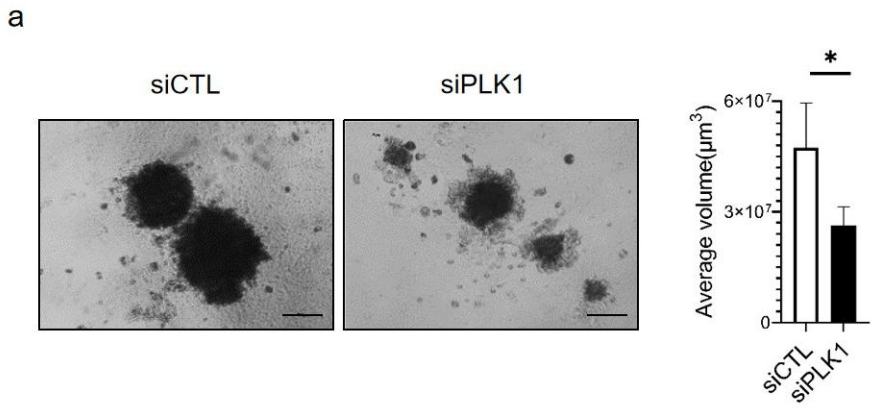

Figure 5. PLK1 knockdown decreased sphere formation abilities of MDA-MB-231 cells **a.** At 72 hours after transfection, sphere formation was examined using 3D Matrigel assays (n=10 spheroids). Scale bar=200μm; Error bars are mean ± SD; Student's *t*-tests. $*p < 0.05$

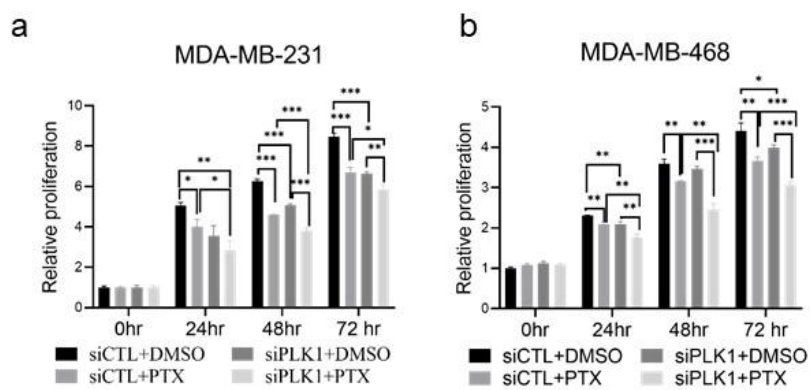

Figure 6. In both MDA-MB-231 and MDA-MB-468 cells, combining si-PLK1 and PTX resulted in increased cell death compared with PTX treatment alone **a, b.** An MTT assay in MDA-

MB-231 and MDA-MB-468 cells after si-PLK1 and PTX treatment. Cells were treated for 72 hours with 10nM PLK1 siRNA, 5nM PTX, and both in combination MTT staining. Error bars are mean ± SD; Mann–Whitney U test. $*p < 0.05$, $**p < 0.01$, and $***p < 0.001$

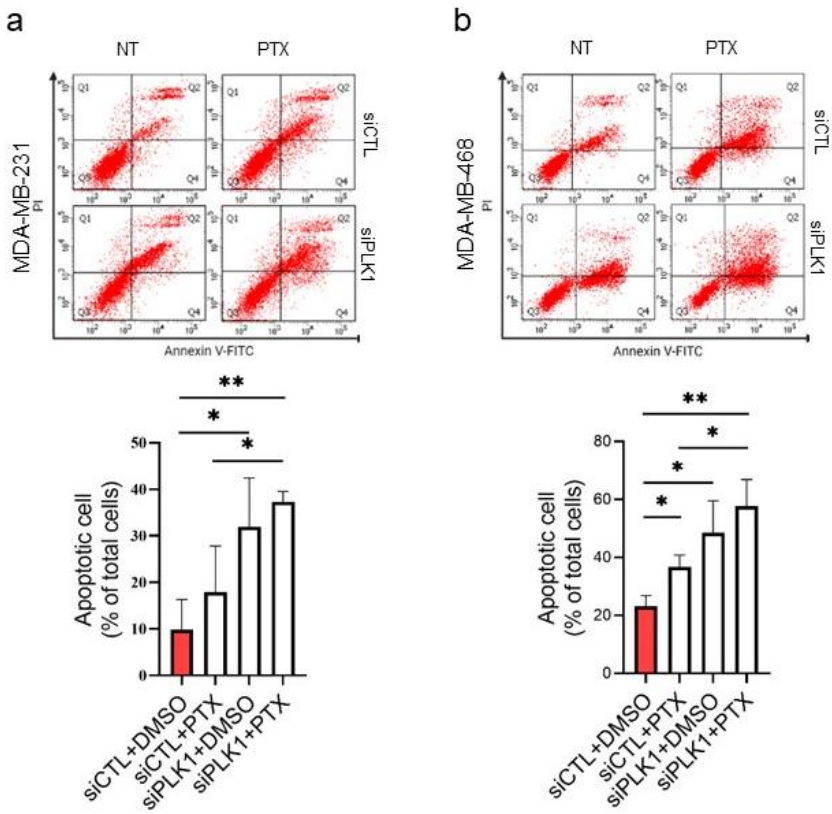

Figure 7. Annexin V assay demonstrated that the combination of si-PLK1 and PTX was associated with increased apoptosis in both cell types **a, b.** Analysis of representative flow cytometry plots of annexin V staining in MDA-MB-231 and MDA-MB-468 cells after si-PLK1 and PTX treatment. Cells were treated for 72 hours with

10nM PLK1 siRNA, 5nM PTX, and both in combination before annexin V staining (n = 3). Error bars are mean ± SD; Student's *t*-tests. $*p < 0.05$, and $**p < 0.01$

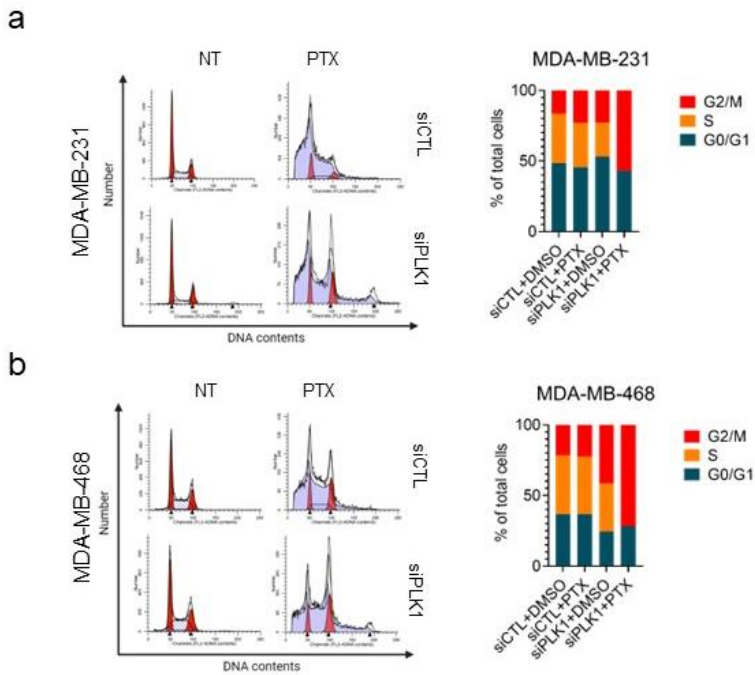

Figure 8. Combination of si-PLK1 and PTX was associated with increased apoptosis in both cell types, which occurred by inducing G2/M cell cycle arrest **a, b.** Cell cycle progression of PLK1 depletion cells was analyzed after PTX treatment. Cells were treated for 72 hours with 10nM PLK1 siRNA, 5nM PTX, and both in combination before PI staining, followed by flow cytometric analysis

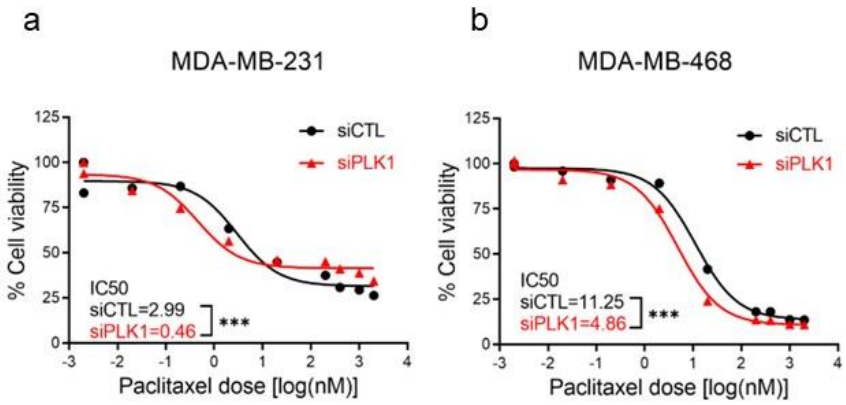

Figure 9. Silencing of PLK1 resulted in a significant reduction in the IC_{50} value of PTX *in vitro* **a, b.** IC_{50} values and response curves against PTX in a panel of MDA-MB-231 and MDA-MB-468 cells according to si-PLK1 treatment (n = 3). Error bars are mean ± SD; Mann–Whitney *U* test. ***$p < 0.001$

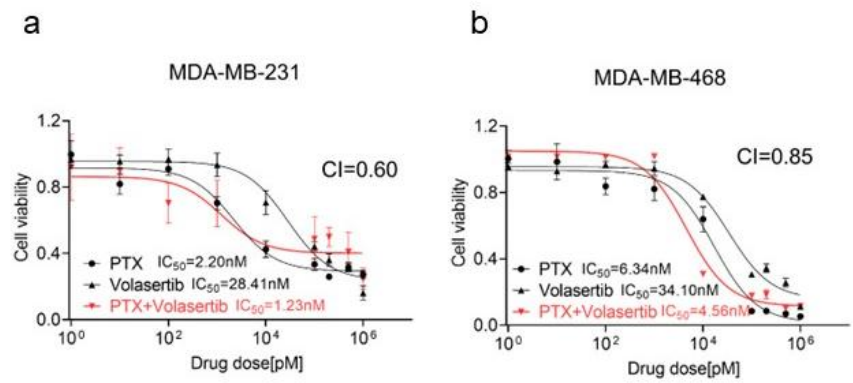

Figure 10. Synergistic effect of the PTX and PLK1 inhibitor volasertib combination treatment on MDA-MB-231 and MDA-MB-468 *in vitro* **a, b.** The combination index (CI) for PTX and PLK1 inhibitor volasertib in a panel of MDA-MB-231 and MDA-MB-468 cells, where CI<1, =1, and >1 indicate synergism, additive

effect, and antagonism, respectively

The prognostic value and clinical relevance of PLK1 as a marker in breast cancer patient specimens

Data from TCGA and METABRIC databases were analyzed to assess the clinical relevance of PLK1 in breast cancer. In both datasets, PLK1 expression was significantly upregulated in tumors compared to normal tissue, with the basal type of breast cancer showing the highest expression level (Figure 11a). Furthermore, patients with high tumor PLK1 expression had poor survival compared to patients with low tumor PLK1 expression in both datasets (Figure 11b).

Data on 45 breast cancer patients who underwent NAC was further analyzed to explore the relationship between PLK1 expression and tumor response to NAC. The objective responses to NAC using the Response Evaluation Criteria in Solid Tumors (RECIST) version 1.1 included complete response (CR), partial response (PR), stable disease (SD), and progressive disease (PD). Despite the small sample size, significantly lower PLK1 expression levels in breast cancer samples were observed in CR patients compared to patients with PR, SD, and PD (Figure 12a). Next, I investigated whether each gene from CRISPR/Cas9 screening identified 28 candidate

genes can predict response in breast cancer in any of PTX-based NAC datasets (GSE41998). Utilizing public data, I found the 11 candidate genes (39.3%) showing the highest expression level in PD (Figure 13a).

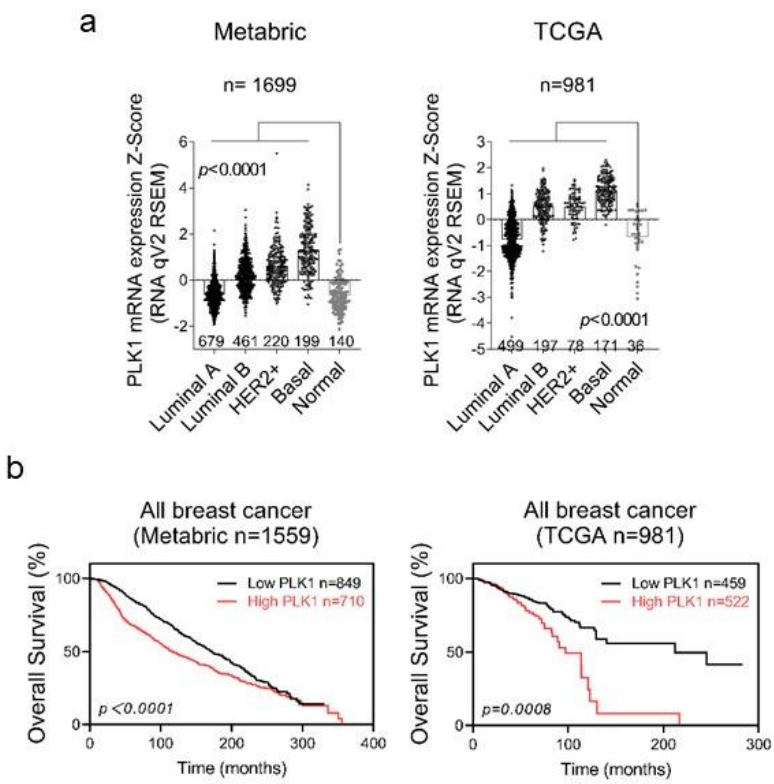

Figure 11. PLK1 expression levels were associated with overall survival (OS) in patients with breast cancer **a.** Expression of PLK1 in the METABRIC BRCA and TCGA breast cancer databases **b.** Overall survival of patients with breast cancer based on PLK1 transcription levels using the Kaplan-Meier plotter online tool

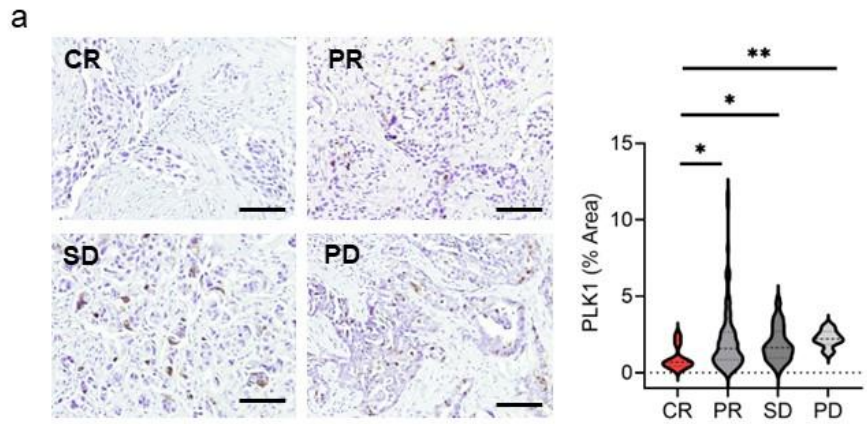

Figure 12. Association of PLK1 with response to neoadjuvant chemotherapy **a.** Representative images of PLK1 staining of tumors derived from 45 patients diagnosed with breast cancer. The area percentage was measured from 3 different images; Scale bars=50μm. Error bars are mean ± SD; Mann–Whitney *U* test. $*p < 0.05$, and $**p < 0.01$

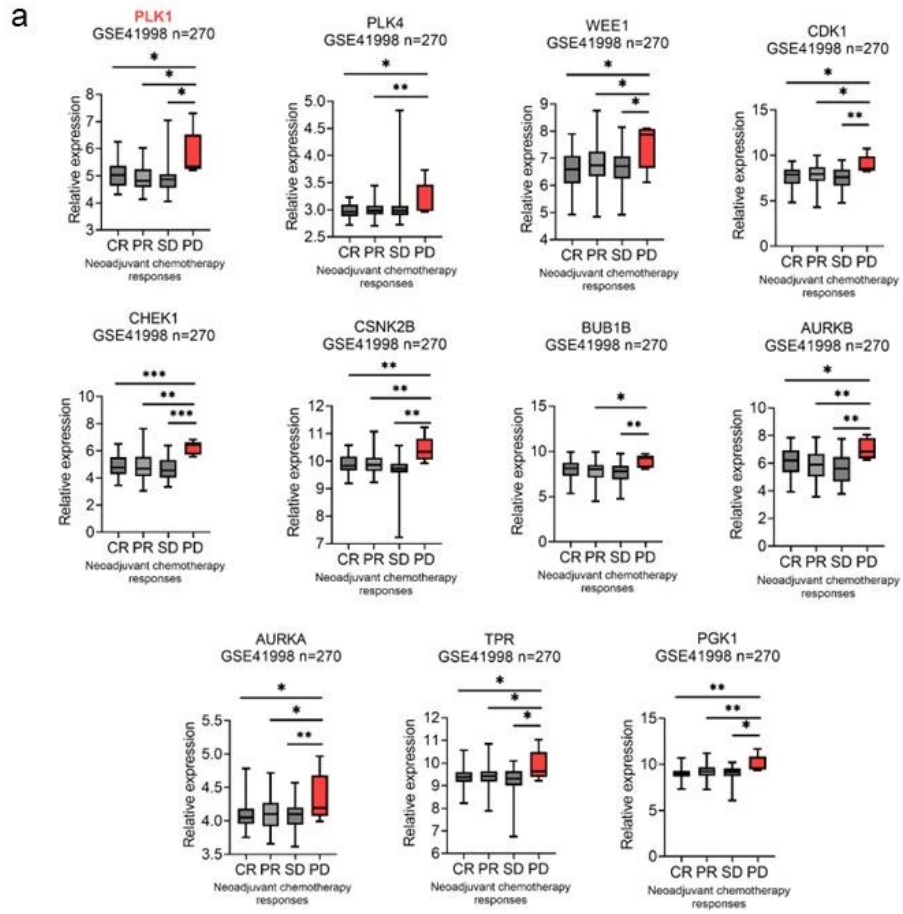

Figure 13. CRISPR/Cas9 screening identified candidate genes associated with response to PTX-based NAC in breast cancer **a.** Expression of 11 candidate genes in complete response (CR), partial response (PR), stable disease (SD), and progressive disease (PD) breast cancer patients (GSE41998) grouped according to their response to PTX-based NAC. Error bars are mean ± SD; Mann–Whitney *U* test. $*p < 0.05$, $**p < 0.01$, and $***p < 0.001$

Discussion

Chemoresistance is a major clinical challenge for TNBC treatment. Therefore, deciphering the molecular mechanisms of chemoresistance and identifying new drugs to synergize with current treatments is very important. Recently, CRISPR-based gene editing techniques have gained popularity as screening tools to probe chemoresistance mechanisms. In the present study, CRISPR/Cas9 screening was performed, which revealed several kinases implicated in PTX resistance in breast cancer, including PLK1. Overall, these data suggest that the use of an anti-PLK1 treatment strategy could potentially combat PTX resistance in breast cancer.

PLK1 plays several roles that enhance cancer cell chemotherapy resistance. In pancreatic cancer, PLK1-dependent DNA replication stress has been found to reduce cellular sensitivity to gemcitabine [42]. In prostate cancer, PLK1 elevation leads to inactivation of PTEN and modulates tumor-promoting metabolism [43]. In castration-resistant prostate cancer (CRPC), PLK1 inhibition causes activation of AR signaling leads to ASI resistance [44]. In addition, Liu et al. [45] reported that PLK1-mediated p53 inactivation contributes to doxorubicin resistance. In the present

study, sgRNA-mediated screening of kinases identified PLK1 as an important factor for PTX resistance in breast cancer cells. Furthermore, PLK1 depletion sensitized breast cancer cells to PTX as indicated by enhanced mitotic arrest and apoptosis. A synergistic effect was also observed between PTX treatment and a PLK1 inhibitor in breast cancer cell lines.

PLK1 is overexpressed in most human cancers and categorized as an oncogene [46]. The oncogenic mechanisms of PLK1 include transcriptional regulation feedback loops, such as the PLK1-p53 negative feedback loop [47, 48] and the PLK1-MYC positive feedback loop [49, 50]. Furthermore, PLK1 inhibits the PTE tumor suppressor PTEN phosphatase, leading to activation of the oncogenic PI3K pathway [43, 51]. On the contrary, some studies report that PLK1 overexpression has tumor suppressive properties through perturbing mitotic processes and increasing the survival of cells with enhanced chromosomal abnormalities [52, 53]. According to gene expression data, PLK1 expression was significantly upregulated in breast tumor tissues, with the basal type showing the highest expression. Furthermore, high PLK1 tumor expression was associated with poor overall survival in breast cancer patients from TCGA and METABRIC datasets.

Next, the relationship between PLK1 expression and pathological

response to NAC in breast cancer patients was explored. NAC is the standard of care for locally advanced TNBC patients, which includes taxane-based and anthracycline-based agents. Regrettably, about 50% of TNBC patients develop resistance and show poor overall survival after NAC [54, 55]. The tumor data of 45 breast cancer patients who underwent NAC was retrospectively analyzed; significantly lower PLK1 expression levels were observed in breast cancer samples from CR patients compared to patients with PR, SD or PD. Utilizing publicly-available data, 11 candidate genes (39.3%) showed the highest expression level in PD breast cancer patient tumors.

This study had several limitations. The small sample size limitedthe statistical power to assess correlations between PLK1 expression and NAC outcome in TNBC patients. Losses to follow-up also limited the survival analysis. Future studies with larger patient cohorts are needed. Nevertheless, these data suggest that PLK1 is a promising biomarker to predict PTX response in breast cancer, highlighting the importance of further mechanistic studies.

Chapter 3.
Targeting PLK1 enhances paclitaxel sensitivity in breast cancer cells

Introduction

Chromosomal instability (CIN) is hallmark of most type cancers [56]. CIN results from segregation errors during mitosis, leading to numerical and structural chromosomal abnormalities in daughter cells [15]. CIN and aneuploidy are related but different traits. Aneuploidies may arise from CIN, and it is characterized by an imbalance at the chromosome level [14]. Although CIN is a common characteristic of human cancer, its role in tumor adaption and evolution is complex [16]. On one hand, high levels of CIN are commonly associated with poor prognosis, metastasis, and oncogene independence in diffuse large B cell lymphoma, breast cancer, and lung cancer [57–59]. Conversely, chromosome missegregation forebodes enhanced sensitivity to cytotoxic and radiation therapies in rectal, breast cancer and glioblastoma tumors [17–19, 60]. These conflicting results suggest a complex role of CIN in cancer progression and response to therapy.

Cell division is a tightly regulated process involving cell cycle

checkpoints that ensure the replication and division of a fully intact genome to daughter cells. However, checkpoint deficiencies, DNA replication stress, and cell division errors can lead to numerical and structural chromosomal abnormalities [61]. Mitotic kinases regulate the cell cycle and thus play a key role in chromosomal segregation. Polo like kinases regulate mitotic stages and associate with mitotic structures, including the centrosome, spindle poles and kinetochores [62].

PLK1 is the hallmark of the PLK family. PLK1 has a crucial role during mitosis and cytokinesis. In bladder cancer, overexpression of PLK1 is significantly associated with CIN and centrosome amplification [63]. PLK1 regulates SAC activity and contributes to CIN in mitosis [64]. PLK1 can also prematurely generate kinetochore–microtubule and contribute to CIN [65]. In addition, PLK1 overexpression induces chromosome missegregation and generates polyploid cells in mouse models [52].

In Chapter 2, PLK1 expression was significantly upregulated in tumor tissues and considered to be oncogenic rather than tumor suppressive. Furthermore, high PLK1–expression in breast tumors was associated with poor survival. In Chapter 3, downregulation of PLK1 and multipolar spindle formation are explored in relation to breast cancer PTX sensitivity.

Materials and Methods

Cell transfection

The pLKO.1-Puro lentiviral vector was used to express short hairpin RNA (shRNA) sequences targeting human PLK1 (point 1, 5′-CACAGTCCTCAATAAAGGCTT-3′; and point 2, 5′-GTTCTTTACTTCTGGCTATAT-3′). Lentiviral pLKO.1-PLK1-shRNA constructs were transfected into HEK-293FT cells using Lipofectamine 3000 (Thermo Fisher Scientific, Waltham, USA). The medium containing the lentivirus was incubated at 37°C and 5% CO2 for 48 hours after transfection. Then, lentiviral supernatant was harvested and used to infect MDA-MB-231 and MDA-MB-468 cells. Cells transduced with pLKO.1-Puro scramble shRNA (shRNA against negative control; sh-NC) were used as negative controls.

Immunohistochemistry

Immunohistochemistry was performed using an IHC staining kit (Agilent, Santa Clara, USA). Tissue sections were deparaffinized in xylene and rehydrated in a series of graded alcohol solutions, and the antigen was retrieved in an antigen unmasking solution (Vector Laboratories, Inc., Burlingame, USA). The sections were then

incubated with 3% hydrogen peroxide to inhibit endogenous peroxidase and blocked with normal goat serum (#AAR-6591-02; ImmunoBioScience Corp., Mukilteo, USA). Subsequently, sections were incubated with primary antibodies at a dilution of 1:1,000 or 1:2,000 at 4°C overnight. Next, the sections were incubated with a secondary anti-rabbit or anti-mouse antibody, followed by incubation with a peroxidase solution. Finally, sections were developed with diaminobenzidine and hydrogen peroxide solution and counterstained with hematoxylin.

Immunofluorescence microscopy

Cells on coverslips were fixed with methanol at -20°C for 30 minutes. Alternatively, cells were extracted using BRB80-T buffer (80 mM PIPES, pH 6.8, 1 mM $MgCl_2$, 5 mM EGTA, and 0.5% Triton X-100) and fixed with 4% paraformaldehyde for 15 minutes at room temperature. Fixed cells were permeabilized and blocked with phosphate-buffered saline (PBS)-BT (1× PBS, 3% BSA, and 0.1% Triton X-100) for 30 minutes at room temperature. The coverslips were then incubated with primary and secondary antibodies diluted in PBS-BT. Images were acquired using stimulated emission depletion (STED) at 3× super-resolution (Leica Microsystems GmbH, Mannheim, Germany) under a Leica TCS SP8 confocal

microscope and a 63× oil immersion lens. Data from all studies were analyzed using the Leica Application Suite X (LAS X) software (Leica Microsystems GmbH, Mannheim, Germany). The primary antibodies used were mouse anti-γ-tubulin (#T6557; Sigma) and rabbit anti-pericentrin (#ab4448; Abcam). The secondary antibodies used were Alexa Fluor 488 and 594 (Invitrogen, Waltham, USA).

Xenograft murine model and drug treatment

MDA-MB-231 cells stably transfected with sh-NC and shPLK1 were injected into the fourth mammary fat pad of 6-week-old athymic nude female mice. The mice were cared for according to the institutional guidelines for animal care. All animal experiments were approved by the Institutional Animal Care and Use Committee of the Seoul National University (No. 18-0127-C1A1). Drug treatment was initiated after the tumors reached approximately 100 mm^3. Mice were randomly divided according to tumor size into four treatment groups (five mice per group): 1) sh-NC group treated with vehicle, 2) sh-NC group treated with PTX, 3) sh-PLK1 group treated with vehicle, and 4) sh-PLK1 group treated with PTX. For each murine xenograft model, either PBS (200 μL/mouse; 5 sh-NC mice, 5 shPLK1 mice) or PTX (15 mg/kg; 5

sh-NC mice, 5 shPLK1 mice) was intraperitoneally (IP) injected twice weekly until tumors reached 1,000 mm^3. The length and width of each tumor were measured using calipers, and the volumes were calculated using the following equation: V = (length × $width^{2)}$/2.

RNA-seq and bioinformatics

RNA sequencing libraries were constructed using the TruSeq Stranded mRNA-seq Prep kit (Illumina, Inc., San Diego, CA, USA) according to the manufacturer's protocol. RNA-seq was performed by Paired-end 101bp RNA sequencing using a Novaseq 6000 system (Illumina, Inc., San Diego, CA, USA). The Differentially Expressed Genes (DEGs) between MDA-MB-231 siPLK1 and siCTL were analyzed by DNA link (Seoul, Korea).

Statistical analysis

GraphPad Prism version 8.02 (GraphPad Software, San Diego, USA) was used to generate graphs and perform statistical tests. For *in vivo* drug responses, multiple *t*-tests to compare tumor volumes.

Results

Whole transcriptome analysis reveals that PLK1 depletion elicits widespread gene expression changes and signaling dysregulation

RNA-sequencing (RNA-Seq) was conducted to identify the transcriptional targets of PLK1. As shown in Figure 14a, differentially expressed genes (DEGs) in PLK1-depleted cells are highlighted in red if decreased than two-fold and highlighted in blue if upregulated more than two-fold. Among the DEGs, 39 upregulation and 66 downregulation genes (p <0.05) are highlighted in green (Figure 14b). Biological functions associated with PLK1-loss were assessed using the Gene Ontology (GO) terms and Kyoto Encyclopedia of Genes and Genomes (KEGG) pathways. As shown in Figure 14c, the downregulated DEGs were mainly enriched in 'telomere organization, DNA replication-dependent nucleosome assembly' (Biological Process, BP), 'structural constituent of chromatin' (Molecular Function, MF) and 'nuclear chromosome' (Cellular Component, CC). Moreover, the top 10 enriched KEGG pathways of common DEGs were identified, including: 'Transcriptional misregulation in cancer'. These significant pathways may lead to chromosome missegregation and increase cell death.

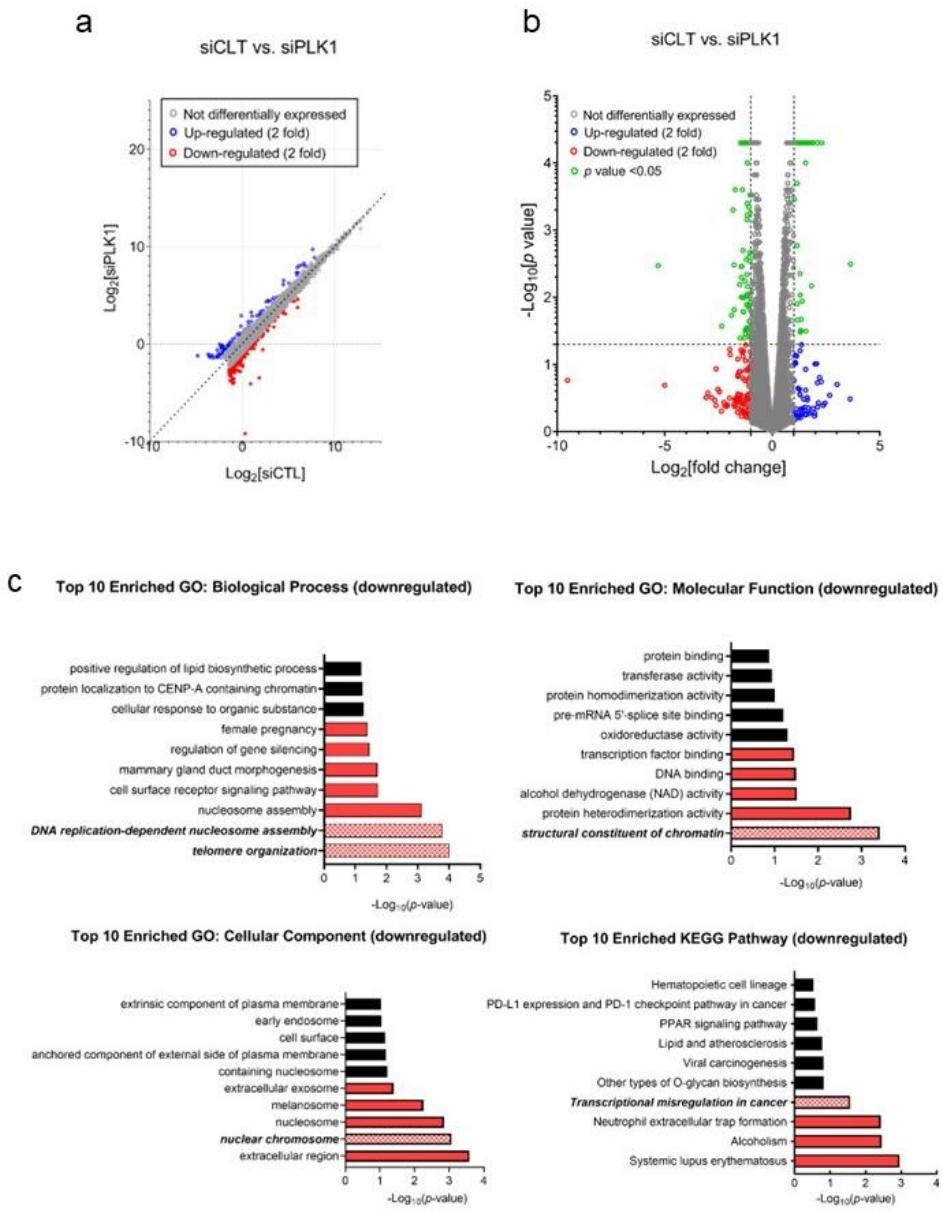

Figure 14. PLK1 depletion leads to de-regulation of general gene expression associated with chromosome missegregation **a, b.** Scatter plot and Volcano plot of DEGs comparing siPLK1 and siCTL-transfected MDA-MB-231 **c.** Top 10 enriched GO and KEGG pathway analyses of DEGs. $p < 0.05$ indicated in red

Increased multipolar spindles and impaired SACs in PLK1-silenced breast cancer cells

Recent studies have suggested that PTX sensitivity depends on the degree of CIN in cancer [8, 9, 13]. To explore the association between PLK1 expression and CIN in breast cancer, I examined multipolar cell division using DNA, centrosome, and microtubule staining (Figure 15a and 16a). As shown in Figure 17a, PTX treatment increased the incidence of multipolar spindles in breast cancer cells. PLK1 silencing resulted in an increased incidence of multipolar spindles. Furthermore, the combined use of si-PLK1 and PTX resulted in a significantly higher incidence of multipolar spindles in MDA-MB-231 cells than from PTX treatment alone (Figure 17b). These data indicate that the downregulation of PLK1 promotes multipolar spindle formation, which can lead to increased PTX sensitivity. Similar to the results of the breast cancer cells (MDA-MB-231 and MDA-MB-468), PLK1-silenced noncancerous cells (MCF10A and WI38) (Figure 18a and b) showed a significantly increased incidence of multipolar spindles (Figure 18c).

Next, I investigated the expression levels of BubR1 and Mad2, which are key regulatory proteins for SAC activity in prometaphase; SAC controls the dynamic interaction between spindle microtubules

and kinetochores [66]. BubR1 expression was upregulated when breast cancer cells were treated with PTX (Figure 19a). In contrast, cells treated with si-PLK1 showed significant downregulation of BubR1 expression, which was not attenuated by the PTX treatment (Figure 19b). Similar findings were observed with Mad2. Furthermore, kinetochore localization of BubR1 was significantly reduced in PLK1-silenced breast cancer cells (Figure 20a and b). These observations suggest that siPLK1 plays a crucial regulatory role in SAC activity, which can lead to CIN by regulating the expression levels of BubR1 and Mad2 in breast cancer cells.

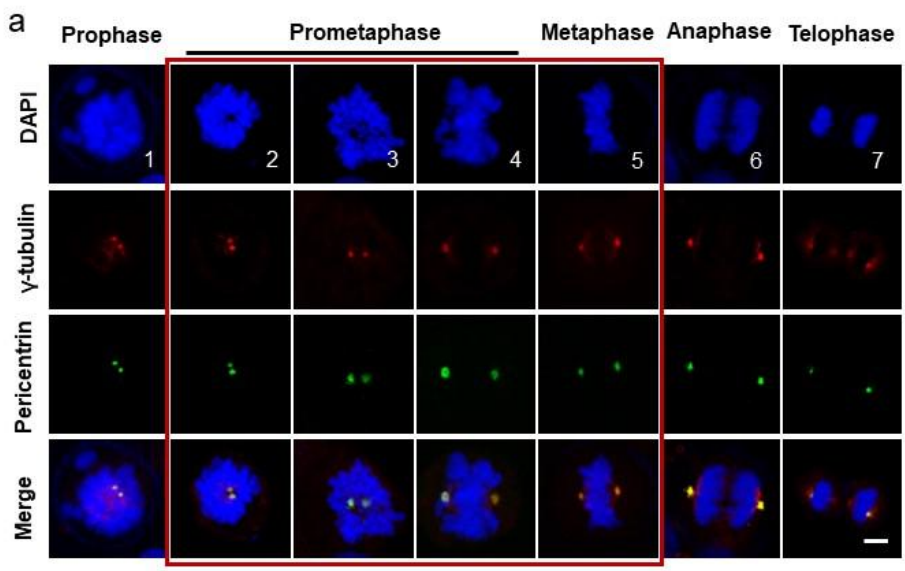

Figure 15. Images of mitotic stages visualized with DNA, centrosome and MTs staining **a.** Mitotic MDA-MB-231 cells in prophase (panel 1), prometaphase (panels 2-4), metaphase (panel

5), anaphase (panel 6), and telophase (panel 7). Images are maximum projections from z stacks of representative cells stained for DNA (DAPI, blue), centrosomes (pericentrin, green), and MTs (γ-tubulin, red). Scale bar=5μm

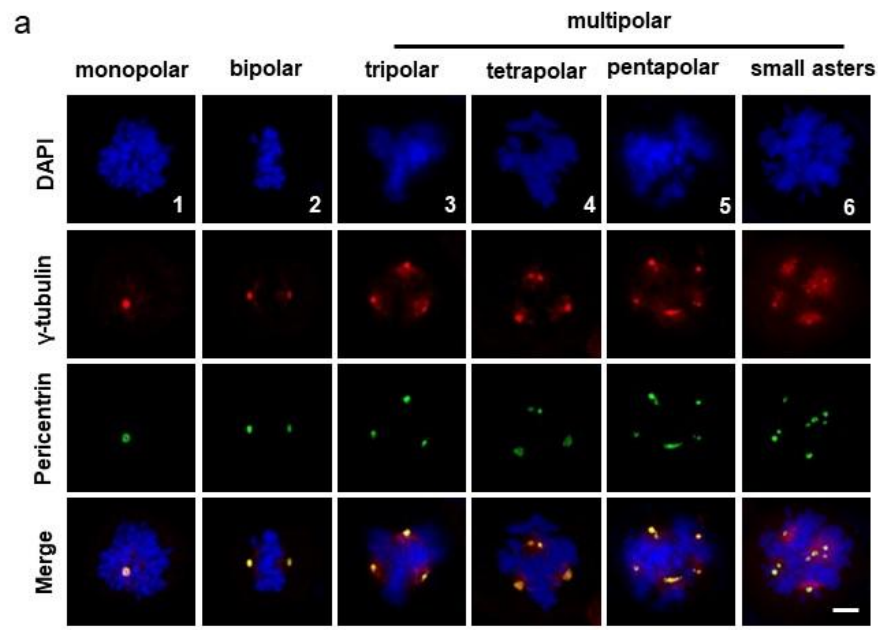

Figure 16. Images of mitotic spindles with the indicated number of poles in MDA-MB-231 and MDA-MB-468 cells after treatment with siPLK1 and PTX **a.** Monopolar spindle (panel 1), bipolar spindle (panel 2), and multipolar spindle (panels 3–6). Scale bar=5μm

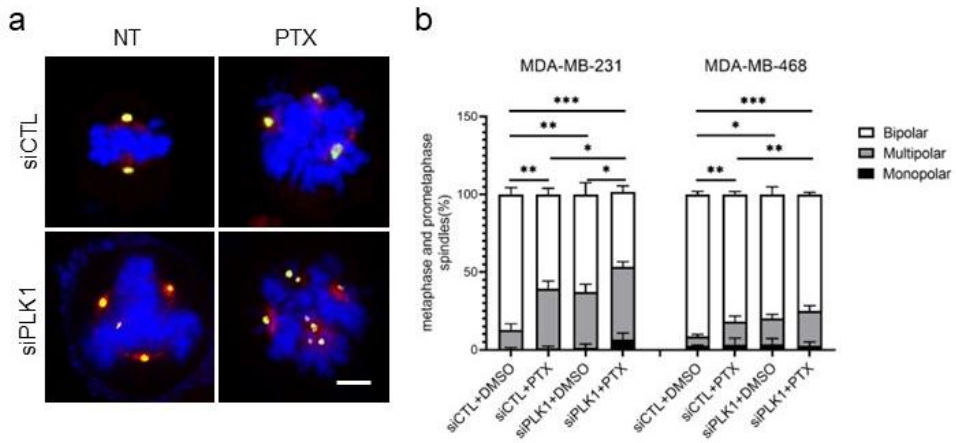

Figure 17. PLK1 silencing resulted in an increased incidence of multipolar spindles **a.** Images of mitotic spindles with the indicated number of poles in breast cancer cells after treatment with siPLK1 and PTX. Images are maximum projections from *z* stacks of representative cells stained for DNA (DAPI, blue), centrosomes (pericentrin, green), and MTs (γ-tubulin, red). Scale bar=5μm **b.** Quantification of multipolar spindles in MDA-MB-231 and MDA-MB-468 cells in prometaphase/metaphase (n>50 cells in each of three replicates). Error bars are mean ± SD (n=3); Student's *t*-tests. $*p < 0.05$, $**p < 0.01$, and $***p < 0.001$

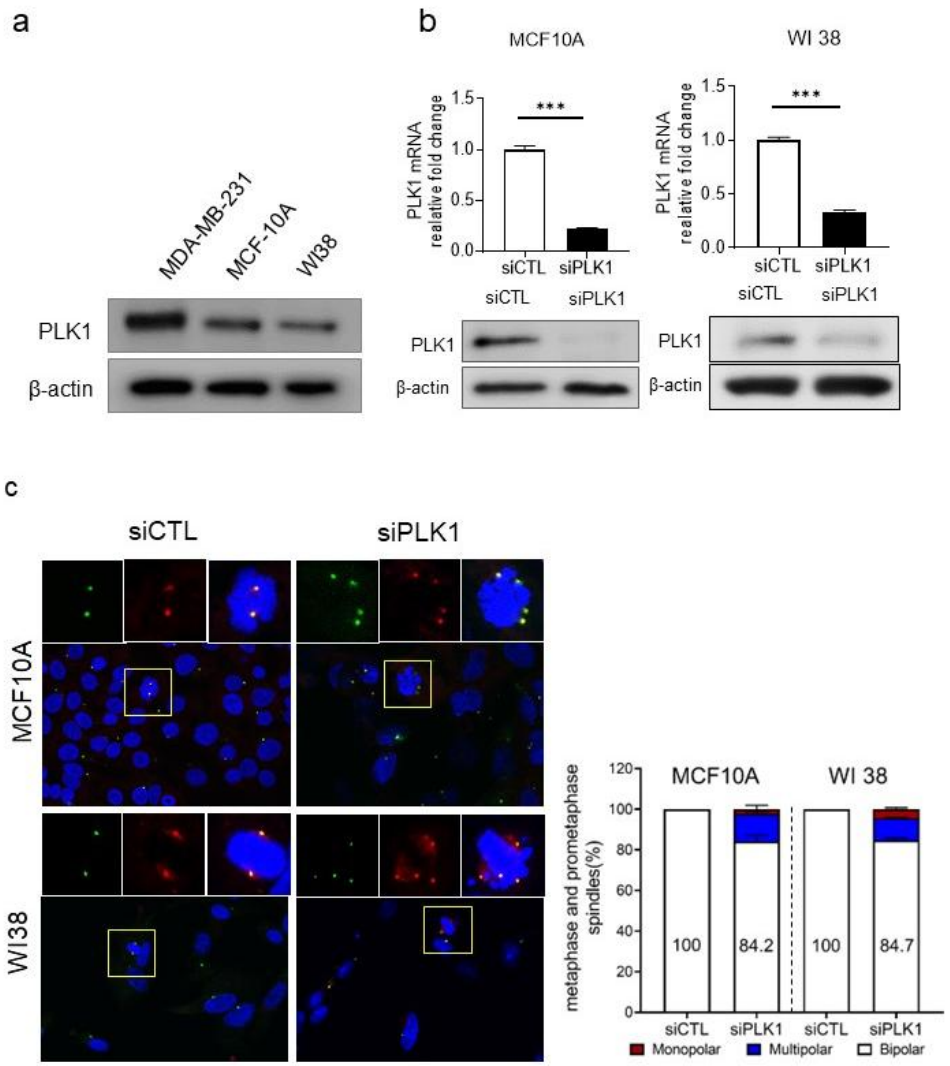

Figure 18. Analysis of PLK1 expression and cell division in normal human cell lines MCF10A and WI38 **a, b.** Western blotting gel images showing the expression levels of PLK1 protein in MCF10A and WI38 (left panel). And mRNA and protein levels of PLK1 after siPLK1 treatment (right panel). Error bars are mean ± SD; Student's *t*−tests. ***$p < 0.001$ **c.** Images of mitotic spindles with the indicated number of poles in multipolar spindles in

prometaphase/metaphase after treatment with siPLK1 (n>30 cells in each of three replicates)

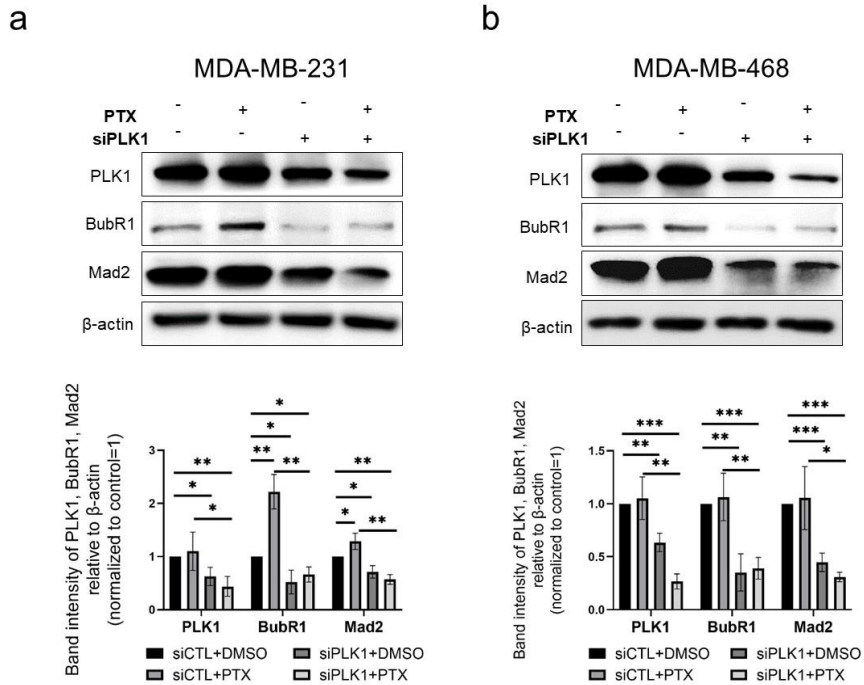

Figure 19. PLK1 depletion plays a crucial regulatory role in SAC activity, and expression levels of BubR1 and Mad2 in breast cancer cells **a, b.** Top: Western blotting of si-PLK1- and PTX-treated MDA-MB-231 and MDA-MB-468 cells. Loading control, β-actin. Bottom: Quantification of BubR1 and Mad2 expression levels normalized to β-actin. Error bars are mean ± SD (n=3); Mann-Whitney *U* test. $*p < 0.05$, $**p < 0.01$, and $***p < 0.001$

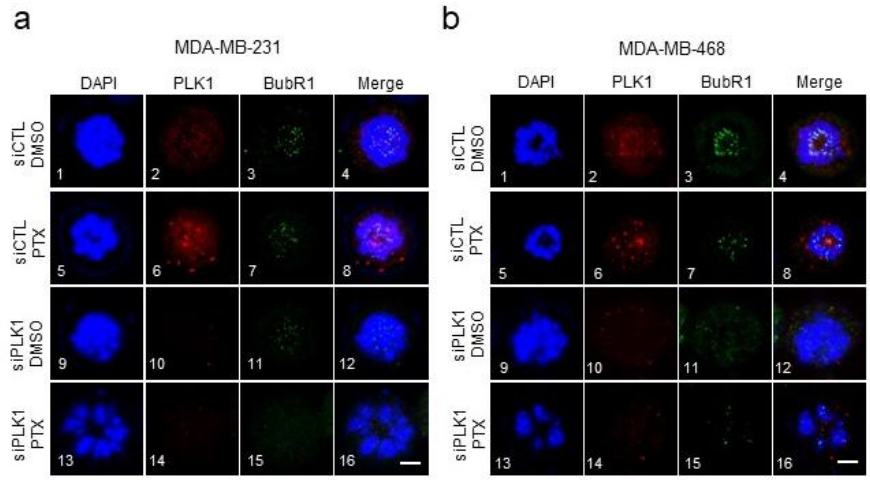

Figure 20. Kinetochore localization of BubR1 was reduced in PLK1-silenced breast cancer cells **a, b.** Localizations of BubR1 and PLK1 in prometaphase shown by immunofluorescence staining. DAPI (blue), BubR1 (green), and PLK1 (red). Scale bar=5μm

Effect of PLK1 on breast cancer growth and PTX resistance *in vivo*

To investigate the role of PLK1 in tumorigenesis, I established stable PLK1 shRNA knockdown MDA-MB-231 and MDA-MB-468 cell lines (Figure 21a). I evaluated xenograft tumor growth in mice by orthotopically injecting cancer cells into the mammary fat pad. PLK1-knockdown cells showed significantly decreased tumor growth rates compared to control cells (non-targeting shRNA; sh-CTL) (Figure 21b). PLK1-knockdown tumor cells showed low PLK1 expression and significantly fewer Ki-67 positive cells

(Figure 22a and b). Next, I treated mice harboring sh-CTL or sh-PLK1 MDA-MB-231 cells with DMSO or PTX, respectively. Treatment with PTX resulted in modest and statistically non-significant tumor growth inhibition in control xenograft tumors (Figure 23a). However, treatment of PLK1-silenced xenograft tumors with PTX resulted in significant inhibition of tumor growth (Figure 23a and b). Similar to the results of the *in vitro* experiments, the PLK1-silenced xenograft tumors showed a significantly increased incidence of multipolar spindles to a similar degree to that of the PTX-treated xenograft tumors (Figure 24a and b). In addition, Mad2 expression was significantly reduced in PLK1-silenced tumors (Figure 25a and b).

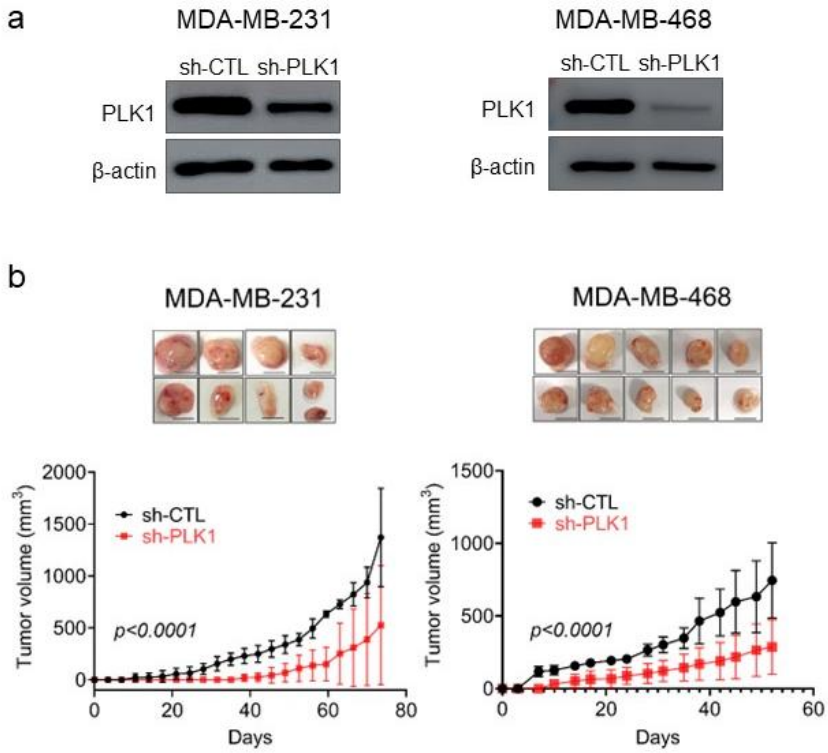

Figure 21. PLK1 depletion suppressed tumor growth in xenograft tumor models **a.** Protein level of PLK1 after sh-PLK1 transfection in MDA-MB-231 and MDA-MB-468 cells **b.** Inhibition of tumor growth generated by xenografted MDA-MB-231 and MDA-MB-468 cell lines in nude mice after silencing of PLK1. Tumor growth curves are shown (MDA-MB-231, n=4 mice/group; MDA-MB-468, n=5 mice/group); two-way ANOVA with Turkey's post hoc test. Scale bars=1cm

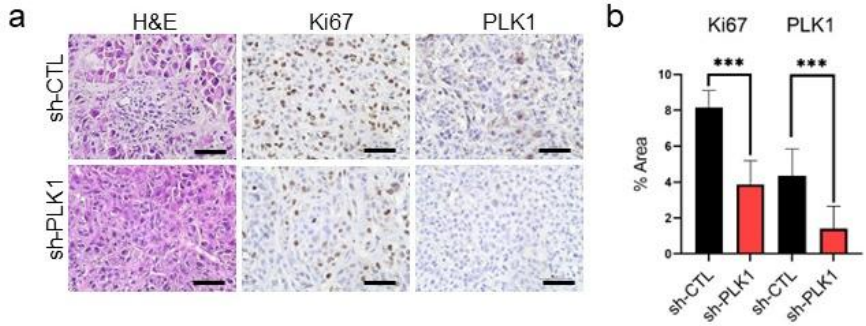

Figure 22. PLK1-knockdown tumor cells showed fewer Ki-67 positive cells **a.** Representative H&E, PLK1 and Ki-67-stained images of tumor and the expression levels of PLK1 and Ki-67 **b.** The area percentage was measured from 10 different images; Scale bars=50μm. Error bars are mean ± SD; Student's *t*-tests. ***p < 0.001

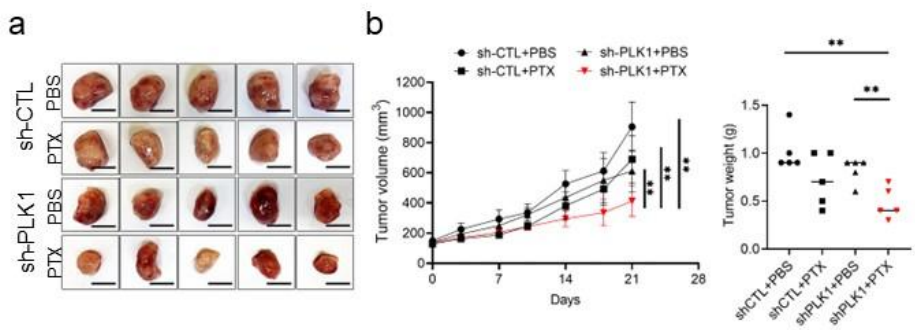

Figure 23. Increased PTX cytotoxicity after PLK1 depletion *in vivo* **a.** PTX treatment of nude mice bearing MDA-MB-231 sh-CTL and sh-PLK1 xenograft tumors. Tumors removed from five mice in each group are shown **b.** Left: Measured tumor volume from days 0 to 21 after treatment plotted versus time. Right: Statistical analysis

of the weights of dissected tumors (n=5 mice/group); Scale bars=1cm. Error bars are mean ± SD; multiple t-testing. $^{**}p < 0.01$

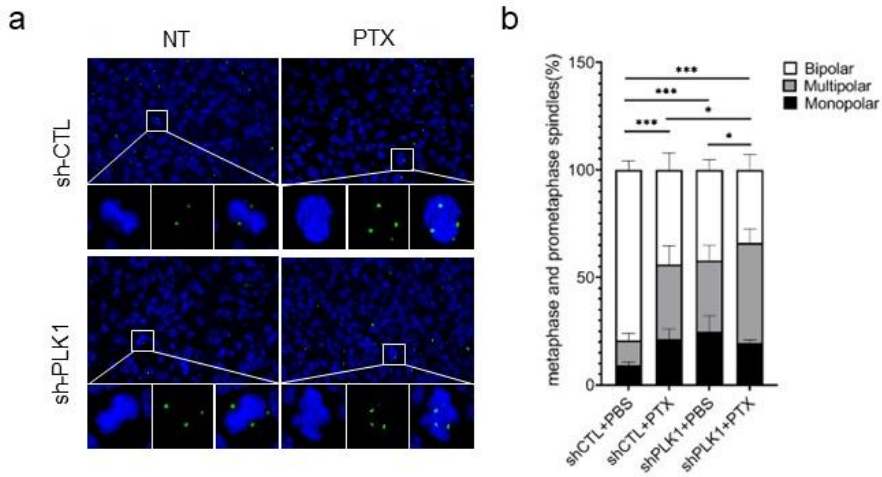

Figure 24. Increased multipolar spindles in PLK1-silenced xenograft tumor models **a.** Images of mitotic spindles with the indicated number of poles in MDA-MB-231 sh-CTL and sh-PLK1 xenograft tumors after PTX treatment **b.** Quantification of multipolar spindles in MDA-MB-231 xenograft tumors (n>30 cells/mice); Error bars are mean ± SD; Mann–Whitney U test. $^{*}p < 0.05$, and $^{***}p < 0.001$

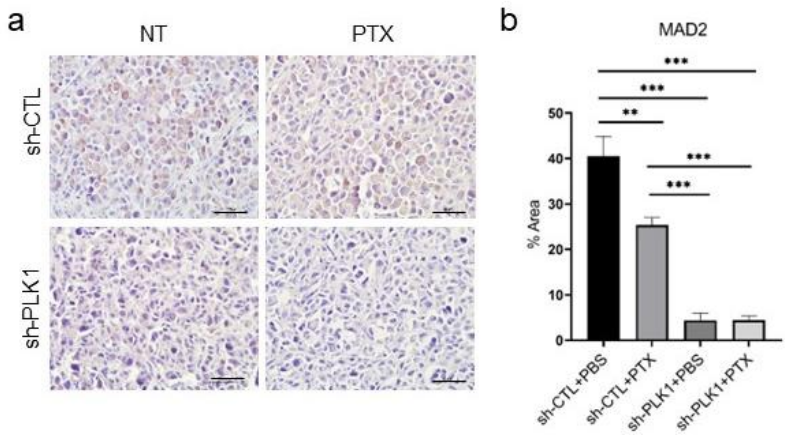

Figure 25. Mad2 expression was reduced in PLK1-silenced tumors

a, b. Representative images of Mad2 staining of tumors derived from MDA-MB-231 with PLK1 depletion and treatment PTX. Scale bars=50μm. Error bars are mean ± SD; Student's *t*-tests. $^{**}p < 0.01$, and $^{***}p < 0.001$

Discussion

In the present study, PLK1 downregulation increased the incidence of multipolar spindles, thereby exacerbating mitotic abnormalities and cell death in response to PTX treatment. My data suggest that PLK1 downregulation affects PTX sensitivity in breast cancer cells by increasing the rate of CIN.

Extensive published data have shown that CIN is associated with PTX sensitivity in breast cancer [12, 13, 67]. CIN has recently been shown to increase PTX sensitivity in breast cancer cells [13]. CIN refers to errors in mitosis, including multipolar spindles, defects in mitotic spindle assembly, and improper kinetochore–microtubule attachment [68]. In cell cultures, mitotic divisions on multipolar spindles result in chromosome missegregation and increase cell death [69]. Genetic ablation of PLK1 or its pharmacological inhibition induces G2/M arrest, creates multipolar cell division, and induces apoptotic cell death [70, 71]. Accordingly, the current study found that PLK1 depletion induced the formation of multipolar spindles and increased the percentage of multipolar cells. However, PLK1 inhibition did not increase PTX–induced multipolar division. Thus, PLK1 silencing before PTX exposure resulted in transient CIN and improved breast cancer sensitivity to

treatment.

My data further demonstrated that PLK1 regulates CIN, which is associated with PTX resistance. PLK1 activity stabilizes kinetochore–microtubule attachments by reducing microtubule dynamics at the kinetochores [72]; however, overactive PLK1 enhances stabilization of microtubules and promotes misattachments, leading to CIN [73]. Furthermore, dysregulation of PLK1 prematurely generates kinetochore–microtubule attachments, leading to CIN on chromosome missegregation [53, 65]. Therefore, dysregulation of PLK1 in either direction results in erroneous kinetochore–microtubule attachments and chromosome missegregation [61]. Additionally, PLK1 can dysregulate mitotic entry and impair mitotic checkpoints, resulting in CIN [74]. Notably, PLK1 depletion impaired SAC, which monitors kinetochore–microtubule attachments. My data suggest that the inhibition of PLK1 weakens the mitotic checkpoint and causes CIN during multipolar division.

My study had several limitations. The distinction between aneuploidy and CIN was first recognized when the former was denoted as a state of abnormal chromosome number and morphology, whereas the latter was defined as chromosome missegregation [15]. The abnormal chromosome number and

morphology of PLK1 depleted cells could not be determined. Although aneuploidy is frequently deleterious to cell fitness, it has a selective advantage in certain tumor environments. Second, mitotic spindles and centrosomes were counted using staining to confirm the presence of CIN. However, the correlation between PLK1 and CIN-associated genes could not be analyzed. There are several methods for measuring CIN, including in situ hybridization [75], flow and DNA image cytometry [76], CIN70 signatures [77], and comparative genomic hybridization [78]. Finally, a time-lapse analysis of cell division was not performed. Analysis of the percentage of cell death in multipolar spindle cells further demonstrated that PLK1-induced multipolar cell division directly resulted in cell death.

Conclusion

In conclusion, my data indicated that PLK1 may induce CIN to improve PTX sensitivity in breast cancer. Targeting PLK1 in PTX-resistant TNBC with CIN is an effective therapeutic strategy. PLK1 can predict response in breast cancer in any of PTX-based NAC.

References

1. Sung H, Ferlay J, Siegel RL, Laversanne M, Soerjomataram I, Jemal A, Bray F: Global Cancer Statistics 2020: GLOBOCAN Estimates of Incidence and Mortality Worldwide for 36 Cancers in 185 Countries. CA Cancer J Clin 2021, 71(3):209-249.

2. Ferlay J, Colombet M, Soerjomataram I, Parkin DM, Pineros M, Znaor A, Bray F: Cancer statistics for the year 2020: An overview. Int J Cancer 2021.

3. Perou CM, Sorlie T, Eisen MB, van de Rijn M, Jeffrey SS, Rees CA, Pollack JR, Ross DT, Johnsen H, Akslen LA et al: Molecular portraits of human breast tumours. Nature 2000, 406(6797):747-752.

4. Waks AG, Winer EP: Breast Cancer Treatment: A Review. JAMA 2019, 321(3):288-300.

5. Rakha EA, Reis-Filho JS, Ellis IO: Basal-like breast cancer: a critical review. J Clin Oncol 2008, 26(15):2568-2581.

6. Senkus E, Kyriakides S, Ohno S, Penault-Llorca F, Poortmans P, Rutgers E, Zackrisson S, Cardoso F, Committee EG: Primary breast cancer: ESMO Clinical Practice Guidelines for diagnosis, treatment and follow-up. Ann Oncol 2015, 26 Suppl 5:v8-30.

7. Cardoso F, Costa A, Norton L, Senkus E, Aapro M, Andre F, Barrios CH, Bergh J, Biganzoli L, Blackwell KL et al: ESO-ESMO 2nd international consensus guidelines for advanced breast cancer (ABC2)dagger. Ann Oncol 2014, 25(10):1871-1888.

8. A'Hern RP, Jamal-Hanjani M, Szasz AM, Johnston SR, Reis-Filho JS, Roylance R, Swanton C: Taxane benefit in breast cancer--a role for grade and chromosomal stability. Nat Rev Clin Oncol 2013, 10(6):357-364.

9. Weaver BA, Cleveland DW: Decoding the links between mitosis, cancer, and chemotherapy: The mitotic checkpoint, adaptation, and cell death. Cancer Cell 2005, 8(1):7-12.

10. Murray S, Briasoulis E, Linardou H, Bafaloukos D, Papadimitriou C: Taxane resistance in breast cancer: mechanisms, predictive biomarkers and circumvention strategies. Cancer Treat Rev 2012, 38(7):890-903.

11. Sudo T, Nitta M, Saya H, Ueno NT: Dependence of paclitaxel sensitivity on a functional spindle assembly checkpoint. Cancer Res 2004, 64(7):2502-2508.

12. Swanton C, Nicke B, Schuett M, Eklund AC, Ng C, Li Q, Hardcastle T, Lee A, Roy R, East P et al: Chromosomal instability determines taxane response. Proc Natl Acad Sci U S A 2009, 106(21):8671-8676.

13. Scribano CM, Wan J, Esbona K, Tucker JB, Lasek A, Zhou AS, Zasadil LM, Molini R, Fitzgerald J, Lager AM et al: Chromosomal instability sensitizes patient breast tumors to multipolar divisions induced by paclitaxel. Sci Transl Med 2021, 13(610):eabd4811.

14. Vasudevan A, Schukken KM, Sausville EL, Girish V, Adebambo OA, Sheltzer JM: Aneuploidy as a promoter and suppressor of malignant growth. Nat Rev Cancer 2021, 21(2):89-103.

15. Bakhoum SF, Cantley LC: The Multifaceted Role of Chromosomal Instability in Cancer and Its Microenvironment. Cell 2018, 174(6):1347-1360.

16. Birkbak NJ, Eklund AC, Li Q, McClelland SE, Endesfelder D, Tan P, Tan IB, Richardson AL, Szallasi Z, Swanton C: Paradoxical relationship between chromosomal instability and survival outcome in cancer. Cancer Res 2011, 71(10):3447-3452.

17. Jamal-Hanjani M, A'Hern R, Birkbak NJ, Gorman P, Gronroos E, Ngang S, Nicola P, Rahman L, Thanopoulou E, Kelly G et al: Extreme chromosomal instability forecasts improved outcome in ER-negative breast cancer: a prospective validation cohort study from the TACT trial. Ann Oncol 2015, 26(7):1340-1346.

18. Roylance R, Endesfelder D, Gorman P, Burrell RA, Sander J,

Tomlinson I, Hanby AM, Speirs V, Richardson AL, Birkbak NJ et al: Relationship of extreme chromosomal instability with long-term survival in a retrospective analysis of primary breast cancer. Cancer Epidemiol Biomarkers Prev 2011, 20(10):2183-2194.

19. Zaki BI, Suriawinata AA, Eastman AR, Garner KM, Bakhoum SF: Chromosomal instability portends superior response of rectal adenocarcinoma to chemoradiation therapy. Cancer 2014, 120(11):1733-1742.

20. Cahill DP, Kinzler KW, Vogelstein B, Lengauer C: Genetic instability and darwinian selection in tumours. Trends Cell Biol 1999, 9(12):M57-60.

21. Bhullar KS, Lagaron NO, McGowan EM, Parmar I, Jha A, Hubbard BP, Rupasinghe HPV: Kinase-targeted cancer therapies: progress, challenges and future directions. Mol Cancer 2018, 17(1):48.

22. Kurata M, Yamamoto K, Moriarity BS, Kitagawa M, Largaespada DA: CRISPR/Cas9 library screening for drug target discovery. J Hum Genet 2018, 63(2):179-186.

23. Lai TC, Fang CY, Jan YH, Hsieh HL, Yang YF, Liu CY, Chang PM, Hsiao M: Kinase shRNA screening reveals that TAOK3 enhances microtubule-targeted drug resistance of breast cancer cells via the NF-kappaB signaling pathway. Cell Commun Signal

2020, 18(1):164.

24. Yu Y, Gaillard S, Phillip JM, Huang TC, Pinto SM, Tessarollo NG, Zhang Z, Pandey A, Wirtz D, Ayhan A et al: Inhibition of Spleen Tyrosine Kinase Potentiates Paclitaxel-Induced Cytotoxicity in Ovarian Cancer Cells by Stabilizing Microtubules. Cancer Cell 2015, 28(1):82-96.

25. Shalem O, Sanjana NE, Hartenian E, Shi X, Scott DA, Mikkelson T, Heckl D, Ebert BL, Root DE, Doench JG et al: Genome-scale CRISPR-Cas9 knockout screening in human cells. Science 2014, 343(6166):84-87.

26. Wang T, Wei JJ, Sabatini DM, Lander ES: Genetic screens in human cells using the CRISPR-Cas9 system. Science 2014, 343(6166):80-84.

27. Chen X, Sun X, Guan J, Gai J, Xing J, Fu L, Liu S, Shen F, Chen K, Li W et al: Rsf-1 Influences the Sensitivity of Non-Small Cell Lung Cancer to Paclitaxel by Regulating NF-kappaB Pathway and Its Downstream Proteins. Cell Physiol Biochem 2017, 44(6):2322-2336.

28. Heyza JR, Lei W, Watza D, Zhang H, Chen W, Back JB, Schwartz AG, Bepler G, Patrick SM: Identification and Characterization of Synthetic Viability with ERCC1 Deficiency in Response to Interstrand Crosslinks in Lung Cancer. Clin Cancer Res

2019, 25(8):2523-2536.

29. Bialk P, Wang Y, Banas K, Kmiec EB: Functional Gene Knockout of NRF2 Increases Chemosensitivity of Human Lung Cancer A549 Cells In Vitro and in a Xenograft Mouse Model. Mol Ther Oncolytics 2018, 11:75-89.

30. Yu J, Zhou J, Xu F, Bai W, Zhang W: High expression of Aurora-B is correlated with poor prognosis and drug resistance in non-small cell lung cancer. Int J Biol Markers 2018, 33(2):215-221.

31. Zitouni S, Nabais C, Jana SC, Guerrero A, Bettencourt-Dias M: Polo-like kinases: structural variations lead to multiple functions. Nat Rev Mol Cell Biol 2014, 15(7):433-452.

32. King SI, Purdie CA, Bray SE, Quinlan PR, Jordan LB, Thompson AM, Meek DW: Immunohistochemical detection of Polo-like kinase-1 (PLK1) in primary breast cancer is associated with TP53 mutation and poor clinical outcom. Breast Cancer Res 2012, 14(2):R40.

33. Maire V, Nemati F, Richardson M, Vincent-Salomon A, Tesson B, Rigaill G, Gravier E, Marty-Prouvost B, De Koning L, Lang G et al: Polo-like kinase 1: a potential therapeutic option in combination with conventional chemotherapy for the management of patients with triple-negative breast cancer. Cancer Res 2013,

73(2):813-823.

34. Burstein HJ, Curigliano G, Loibl S, Dubsky P, Gnant M, Poortmans P, Colleoni M, Denkert C, Piccart-Gebhart M, Regan M et al: Estimating the benefits of therapy for early-stage breast cancer: the St. Gallen International Consensus Guidelines for the primary therapy of early breast cancer 2019. Ann Oncol 2019, 30(10):1541-1557.

35. Marra A, Curigliano G: Adjuvant and Neoadjuvant Treatment of Triple-Negative Breast Cancer With Chemotherapy. Cancer J 2021, 27(1):41-49.

36. Park S, Kim TM, Cho SY, Kim S, Oh Y, Kim M, Keam B, Kim DW, Heo DS: Combined blockade of polo-like kinase and pan-RAF is effective against NRAS-mutant non-small cell lung cancer cells. Cancer Lett 2020, 495:135-144.

37. Doench JG, Fusi N, Sullender M, Hegde M, Vaimberg EW, Donovan KF, Smith I, Tothova Z, Wilen C, Orchard R et al: Optimized sgRNA design to maximize activity and minimize off-target effects of CRISPR-Cas9. Nat Biotechnol 2016, 34(2):184-191.

38. Li W, Xu H, Xiao T, Cong L, Love MI, Zhang F, Irizarry RA, Liu JS, Brown M, Liu XS: MAGeCK enables robust identification of essential genes from genome-scale CRISPR/Cas9 knockout screens.

Genome Biol 2014, 15(12):554.

39. McMillan KS, McCluskey AG, Sorensen A, Boyd M, Zagnoni M: Emulsion technologies for multicellular tumour spheroid radiation assays. Analyst 2016, 141(1):100-110.

40. Eisenhauer EA, Therasse P, Bogaerts J, Schwartz LH, Sargent D, Ford R, Dancey J, Arbuck S, Gwyther S, Mooney M et al: New response evaluation criteria in solid tumours: revised RECIST guideline (version 1.1). Eur J Cancer 2009, 45(2):228-247.

41. Chou TC: Theoretical basis, experimental design, and computerized simulation of synergism and antagonism in drug combination studies. Pharmacol Rev 2006, 58(3):621-681.

42. Song B, Liu XS, Rice SJ, Kuang S, Elzey BD, Konieczny SF, Ratliff TL, Hazbun T, Chiorean EG, Liu X: Plk1 phosphorylation of orc2 and hbo1 contributes to gemcitabine resistance in pancreatic cancer. Mol Cancer Ther 2013, 12(1):58-68.

43. Li Z, Li J, Bi P, Lu Y, Burcham G, Elzey BD, Ratliff T, Konieczny SF, Ahmad N, Kuang S et al: Plk1 phosphorylation of PTEN causes a tumor-promoting metabolic state. Mol Cell Biol 2014, 34(19):3642-3661.

44. Zhang Z, Hou X, Shao C, Li J, Cheng JX, Kuang S, Ahmad N, Ratliff T, Liu X: Plk1 inhibition enhances the efficacy of androgen signaling blockade in castration-resistant prostate cancer. Cancer

Res 2014, 74(22):6635-6647.

45. Liu XS, Li H, Song B, Liu X: Polo-like kinase 1 phosphorylation of G2 and S-phase-expressed 1 protein is essential for p53 inactivation during G2 checkpoint recovery. EMBO Rep 2010, 11(8):626-632.

46. de Carcer G: The Mitotic Cancer Target Polo-Like Kinase 1: Oncogene or Tumor Suppressor? Genes (Basel) 2019, 10(3).

47. McKenzie L, King S, Marcar L, Nicol S, Dias SS, Schumm K, Robertson P, Bourdon JC, Perkins N, Fuller-Pace F et al: p53-dependent repression of polo-like kinase-1 (PLK1). Cell Cycle 2010, 9(20):4200-4212.

48. Ando K, Ozaki T, Yamamoto H, Furuya K, Hosoda M, Hayashi S, Fukuzawa M, Nakagawara A: Polo-like kinase 1 (Plk1) inhibits p53 function by physical interaction and phosphorylation. J Biol Chem 2004, 279(24):25549-25561.

49. Xiao D, Yue M, Su H, Ren P, Jiang J, Li F, Hu Y, Du H, Liu H, Qing G: Polo-like Kinase-1 Regulates Myc Stabilization and Activates a Feedforward Circuit Promoting Tumor Cell Survival. Mol Cell 2016, 64(3):493-506.

50. Ren Y, Bi C, Zhao X, Lwin T, Wang C, Yuan J, Silva AS, Shah BD, Fang B, Li T et al: PLK1 stabilizes a MYC-dependent kinase network in aggressive B cell lymphomas. J Clin Invest 2018,

128(12):5517-5530.

51. Maehama T, Dixon JE: The tumor suppressor, PTEN/MMAC1, dephosphorylates the lipid second messenger, phosphatidylinositol 3,4,5-trisphosphate. J Biol Chem 1998, 273(22):13375-13378.

52. de Carcer G, Venkateswaran SV, Salgueiro L, El Bakkali A, Somogyi K, Rowald K, Montanes P, Sanclemente M, Escobar B, de Martino A et al: Plk1 overexpression induces chromosomal instability and suppresses tumor development. Nat Commun 2018, 9(1):3012.

53. Raab M, Sanhaji M, Matthess Y, Horlin A, Lorenz I, Dotsch C, Habbe N, Waidmann O, Kurunci-Csacsko E, Firestein R et al: PLK1 has tumor-suppressive potential in APC-truncated colon cancer cells. Nat Commun 2018, 9(1):1106.

54. Foulkes WD, Smith IE, Reis-Filho JS: Triple-negative breast cancer. N Engl J Med 2010, 363(20):1938-1948.

55. Liedtke C, Mazouni C, Hess KR, Andre F, Tordai A, Mejia JA, Symmans WF, Gonzalez-Angulo AM, Hennessy B, Green M et al: Response to neoadjuvant therapy and long-term survival in patients with triple-negative breast cancer. J Clin Oncol 2008, 26(8):1275-1281.

56. Nicholson JM, Cimini D: Cancer karyotypes: survival of the

fittest. Front Oncol 2013, 3:148.

57. Bakhoum SF, Danilova OV, Kaur P, Levy NB, Compton DA: Chromosomal instability substantiates poor prognosis in patients with diffuse large B-cell lymphoma. Clin Cancer Res 2011, 17(24):7704-7711.

58. Bakhoum SF, Ngo B, Laughney AM, Cavallo JA, Murphy CJ, Ly P, Shah P, Sriram RK, Watkins TBK, Taunk NK et al: Chromosomal instability drives metastasis through a cytosolic DNA response. Nature 2018, 553(7689):467-472.

59. Sotillo R, Schvartzman JM, Socci ND, Benezra R: Mad2-induced chromosome instability leads to lung tumour relapse after oncogene withdrawal. Nature 2010, 464(7287):436-440.

60. Bakhoum SF, Kabeche L, Wood MD, Laucius CD, Qu D, Laughney AM, Reynolds GE, Louie RJ, Phillips J, Chan DA et al: Numerical chromosomal instability mediates susceptibility to radiation treatment. Nat Commun 2015, 6:5990.

61. Cunningham CE, MacAuley MJ, Vizeacoumar FS, Abuhussein O, Freywald A, Vizeacoumar FJ: The CINs of Polo-Like Kinase 1 in Cancer. Cancers (Basel) 2020, 12(10).

62. Nigg EA: Mitotic kinases as regulators of cell division and its checkpoints. Nat Rev Mol Cell Biol 2001, 2(1):21-32.

63. Yamamoto Y, Matsuyama H, Kawauchi S, Matsumoto H,

Nagao K, Ohmi C, Sakano S, Furuya T, Oga A, Naito K et al: Overexpression of polo-like kinase 1 (PLK1) and chromosomal instability in bladder cancer. Oncology 2006, 70(3):231-237.

64. Ikeda M, Tanaka K: Plk1 bound to Bub1 contributes to spindle assembly checkpoint activity during mitosis. Sci Rep 2017, 7(1):8794.

65. Dumitru AMG, Rusin SF, Clark AEM, Kettenbach AN, Compton DA: Cyclin A/Cdk1 modulates Plk1 activity in prometaphase to regulate kinetochore-microtubule attachment stability. Elife 2017, 6.

66. Khodjakov A, Pines J: Centromere tension: a divisive issue. Nat Cell Biol 2010, 12(10):919-923.

67. Lukow DA, Sausville EL, Suri P, Chunduri NK, Wieland A, Leu J, Smith JC, Girish V, Kumar AA, Kendall J et al: Chromosomal instability accelerates the evolution of resistance to anti-cancer therapies. Dev Cell 2021, 56(17):2427-2439 e2424.

68. Giam M, Rancati G: Aneuploidy and chromosomal instability in cancer: a jackpot to chaos. Cell Div 2015, 10:3.

69. Ganem NJ, Godinho SA, Pellman D: A mechanism linking extra centrosomes to chromosomal instability. Nature 2009, 460(7252):278-282.

70. Lens SM, Voest EE, Medema RH: Shared and separate

functions of polo-like kinases and aurora kinases in cancer. Nat Rev Cancer 2010, 10(12):825-841.

71. Wachowicz P, Fernandez-Miranda G, Marugan C, Escobar B, de Carcer G: Genetic depletion of Polo-like kinase 1 leads to embryonic lethality due to mitotic aberrancies. Bioessays 2016, 38 Suppl 1:S96-S106.

72. Liu D, Davydenko O, Lampson MA: Polo-like kinase-1 regulates kinetochore-microtubule dynamics and spindle checkpoint silencing. J Cell Biol 2012, 198(4):491-499.

73. Bakhoum SF, Thompson SL, Manning AL, Compton DA: Genome stability is ensured by temporal control of kinetochore-microtubule dynamics. Nat Cell Biol 2009, 11(1):27-35.

74. Simonetti G, Bruno S, Padella A, Tenti E, Martinelli G: Aneuploidy: Cancer strength or vulnerability? Int J Cancer 2019, 144(1):8-25.

75. Speicher MR, Carter NP: The new cytogenetics: blurring the boundaries with molecular biology. Nat Rev Genet 2005, 6(10):782-792.

76. Darzynkiewicz Z, Halicka HD, Zhao H: Analysis of cellular DNA content by flow and laser scanning cytometry. Adv Exp Med Biol 2010, 676:137-147.

77. Habermann JK, Doering J, Hautaniemi S, Roblick UJ,

Bundgen NK, Nicorici D, Kronenwett U, Rathnagiriswaran S, Mettu RK, Ma Y et al: The gene expression signature of genomic instability in breast cancer is an independent predictor of clinical outcome. Int J Cancer 2009, 124(7):1552-1564.

78. Pinkel D, Albertson DG: Array comparative genomic hybridization and its applications in cancer. Nat Genet 2005, 37 Suppl:S11-17.

79. Quan M, Oh Y, Cho SY, Kim JH, Moon HG: Polo-Like Kinase 1 Regulates Chromosomal Instability and Paclitaxel Resistance in Breast Cancer Cells. J Breast Cancer. 2022, 25(3):178-192.

국문 초록

염색체 불안정성은 세포 간 유전적 이질성에 기여하며 유방암에서 파클리탁셀 저항성과 관련되어 있으므로, 본 연구에서는 유사분열 과정의 중요한 조절인자인 PLK1 유전자가 유방암에서 파클리탁셀 내성에 미치는 영향과 예측 바이오마커로서 유용성에 대해 탐색하였다.

1장에서는 암세포의 항암제 저항성 현상에 대한 일반적인 개요를 설명한다. 파클리탁셀은 삼중 음성 유방암에서 일반적으로 사용되는 세포독성 항암제이며, 미세소관 형성과 다핵화를 통해 암세포 사멸을 유도한다. 최근 유방암 염색체 불안정화가 심해질수록 파클리탁셀에 좋은 반응을 유도한다는 새로운 연구결과가 보고된 바 있다. 그러나, 염색체 불안정화는 종양의 진행과 전이를 촉진시킨다는 실험결과가 여러 연구에서 기존에 제시된 바 있다. 이처럼 염색체 불안정화가 암세포에 미치는 모순된 결과는 염색체 불안정성은 그 최적 상태에서는 종양 진행을 촉진할 수 있으나, 그 범위 외에서는 암세포 생존을 방해할 수 있다는 가능성을 제시한다. 이런 연구결과를 토대로 본 연구에서는 염색체 불안정화에 삼중음성 유방암에서 항암제 내성에 어떻게 관여하는지를 탐구하고자 한다.

2장에서는 유방암 세포에서 파클리탁셀 저항성과 관련된 유전자를 kinome-wide CRISPR/Cas9 스크리닝을 통해 발굴하는 과정과 그 후보유전자 중 선택된 PLK1이 삼중음성유방암에서 가지는 역할을 실험적

으로 증명한 결과를 제시하였다. 유방암 세포에 대한 PLK1의 효과를 확인하기 위해 유방암 세포주를 이용하여 세포 증식 및 세포 사멸 분석을 진행하였고, PLK1 억제는 *in vitro*에서 MDA-MB-231 및 MDA-MB-468 세포의 증식을 억제하였고, 유방암 세포의 파클리탁셀에 대한 반응성을 향상시킴을 확인하였다. 또한, 공개된 유방암 유전체 데이터를 분석하여 PLK1의 발현정도와 환자의 생존율과의 연관성을 확인하였다. 이 결과를 토대로 PLK1 표적화는 파클리탁셀 내성 유방암에 대한 효과적인 치료 전략이 될 수 있고, 유방암 환자에서 파클리탁셀 기반 항암치료에서 반응성을 예측하는 바이오마커로 사용될 수 있다는 가능성을 확인하였다.

3장에서는 유방암 세포에서 PLK1이 파클리탁셀 저항성에 관여하는 생물학적 기전을 염색체 불안정성을 조절하는 기능을 통해 설명하였다. RNA sequencing 실험을 통해 PLK1을 억제한 유방암세포에서 염색체 이상분열 유전자의 활성도가 감소하는 것을 확인할 수 있었다. 이후 세포분열 과정을 관찰하는 실험을 통해 PLK1 억제가 다극 방추체의 형성을 유도하고 다극성 세포의 비율을 증가시키는 과정을 통해 정상적인 세포분열과정을 저해하는 현상을 관찰하였고, 세포분열의 조절에 필수적인 BubR1 및 Mad2의 발현 저하 및 BubR1의 kinetochore localization의 감소를 확인하였다. 동물실험에서도 PLK1 저하는 생체내 MDA-MB-231 및 MDA-MB-468 세포의 증식을 억제하였고, MDA-MB-231 이종이식 마우스 모델에서 파클리탁셀 약물 반응성을 증가시키는 것을

확인하였다. 동시에 종양조직에서도 PLK1 억제는 다극성 세포의 비율을 유의하게 증가시키는 효과를 보였다. 이런 결과를 토대로 PLK1 저하가 염색체 불안정 및 다극방추체 형성을 조절하여 파클리탁셀 반응성에 관여한다는 기전을 제시할 수 있었다.

이 논문의 일부 내용은 논문에 인용된 바와 같이 학술지(Journal of Breast Cancer)에 발표 되었다[79].

주요어: 유방암, CRISPR/Cas9, 파클리탁셀, PLK1, 방추극, 염색체 불안정성

학번: 2020-35134